



# VCU

Virginia Commonwealth University  
VCU Scholars Compass

---

Theses and Dissertations

Graduate School

---

1998

## Immunocytochemical Study of Apoptosis Signaling In Nb2 Lymphoma Cells

Angelo P. Guanzon

Follow this and additional works at: <https://scholarscompass.vcu.edu/etd>



Part of the [Physiology Commons](#)

© The Author

---

Downloaded from

<https://scholarscompass.vcu.edu/etd/4691>

This Thesis is brought to you for free and open access by the Graduate School at VCU Scholars Compass. It has been accepted for inclusion in Theses and Dissertations by an authorized administrator of VCU Scholars Compass. For more information, please contact [libcompass@vcu.edu](mailto:libcompass@vcu.edu).

Virginia Commonwealth University  
School of Medicine

This is to certify that the thesis prepared by Angelo Guanzon entitled  
"Immunocytochemical Study of Apoptosis Signaling in Nb2 Lymphoma Cells" has  
been approved by his committee as satisfactory completion of the thesis requirement  
for the degree of Master of Science.


  
Raphael Witorsch, Ph.D., Director of Thesis

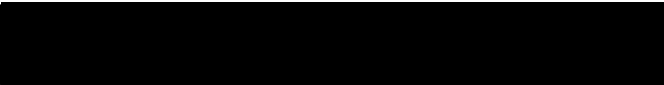
  
Joseph Feher, Ph.D., School of Medicine

  
John Gilder, Ph.D., School of Medicine

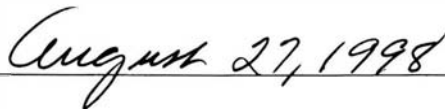
  
Joseph Liberti, Ph.D., School of Medicine

  
Margaret Boadle-Biber, Ph.D., Department Chairman

  
Hermes A. Kontos, M.D., Ph.D., Vice-President for Health Sciences  
And Dean, School of Medicine

  
Jack L. Haar, Ph.D., Dean, School of Graduate Studies

Date

  
August 27, 1998

Immunocytochemical Study of Apoptosis Signaling  
In Nb2 Lymphoma Cells

A thesis submitted in partial fulfillment of the requirements for the degree of Master of  
Science at Virginia Commonwealth University.

By

Angelo P. Guanzon  
B.A. University of Virginia  
Charlottesville, VA 1993

Director: Raphael J. Witorsch, Ph.D.  
Professor  
Department of Physiology

Medical College of Virginia  
Virginia Commonwealth University  
Richmond, Virginia  
August, 1998

## **DEDICATION**

To my family

## ACKNOWLEDGEMENTS

First and foremost, I would like to express my heart-felt gratitude to my advisor Dr. Raphael J. Witorsch for his ever-present encouragement and guidance through out my years at VCU/MCV. I consider it an honor and a pleasure to have worked with such a scholar and a gentleman. In his laboratory, he taught me that enjoyment and laughter could be and should be an integral part of any work environment. I will treasure his friendship always.

I would also like to thank Suhas Badarinath for his friendship and collaborative efforts in lab.

Furthermore, I would like to thank the members of my thesis committee, Dr. Joseph Feher, Dr. Jack Grider and Dr. Joseph Liberti, for their time and efforts on my behalf.

I would also like to thank Ashley Thompson for her friendship, encouragement and support. Through out these past several years, her insights have helped to make me a more complete and conscientious individual.

Lastly, I owe a debt of gratitude for my loving and caring family. Without their love and support, none of my accomplishments could ever have been achieved. Thanks for always being there for me, through the good times and the bad (Pat, Cesar, Michael, Matthew, Mitchell, Clarita and Milagros).

## TABLE OF CONTENTS

	Page
LIST OF TABLES.....	vi
LIST OF FIGURES.....	vii
LIST OF ABBREVIATIONS.....	viii
ABSTRACT.....	ix
1. CHAPTER 1- INTRODUCTION.....	1
1.1- BACKGROUND.....	1
1.2- PURPOSE OF STUDY.....	16
2. CHAPTER 2- MATERIALS AND METHODS.....	18
2.1- Maintenance of Nb2 Lymphoma Cells.....	18
2.2- Chronic (24-Hour) Dex Cytolytic Assay, Acute (Time Point) Dex Cytolytic Assay and Dex-Prl Co-Incubation Assay.....	19
2.3- Cell Fixation.....	21
2.4- TUNEL (Tdt-dependent dUTP-biotin Nick End Labeling) Assay.....	21
2.5- Immunocytochemistry.....	22
2.6- Confirmation of Polyclonal Rabbit Antibody Specificity via Antibody Absorption.....	25
2.7- Photography.....	25
2.8- Cell Quantification.....	26

2.9- Statistics .....	26
3. CHAPTER 3- RESULTS.....	27
3.1- Morphology of Nb2 Lymphoma Cells.....	27
3.2- Hormone Responsiveness to Dex $\pm$ Prl Treatment of Log Phase Nb2 Cells as Measured by Trypan Blue Exclusion and the TUNEL Assay.....	27
3.3- Hormone Responsiveness of Synchronized Nb2 Cells to Dex $\pm$ Prl as Measured by Trypan Blue Exclusion and the TUNEL Assay.....	31
3.4- Immunocytochemistry and Antibody Absorption.....	38
3.5- Examination of the Immunocytological Changes in Antibody Staining in Response to Dex Time Course Assay.....	46
4. CHAPTER 4- DISCUSSION.....	59
5. LIST OF REFERENCES.....	69
6. VITA.....	75

**LIST OF TABLES**

Table	Page
1. The Effects of DMSO and Dex Treatment on NB2 Lymphoma Cells after 0, 1, 2, 4, 6 and 8 Hour Incubation Periods.....	36
2. Immunocytochemical Quantification of Nb2 Lymphoma Cells Stained for Anti-GR after DMSO and Dex Treatment for Various Incubation Periods.....	55
3. Immunocytochemical Quantification of Nb2 Lymphoma Cells Stained for Anti-STAT5B after DMSO and Dex Treatment for Various Incubation Periods.....	56
4. Immunocytochemical Quantification of Nb2 Lymphoma Cells Stained for Anti-NFkB after DMSO and Dex Treatment for Various Incubation Periods.....	57
5. Immunocytochemical Quantification of Nb2 Lymphoma Cells Stained for Anti-IkBa after DMSO and Dex Treatment for Various Incubation Periods.....	58



## LIST OF FIGURES

Figure	Page
1. Photomicrograph of Nb2 Lymphoma Cells Stained With Wright Modified Geimsa Stain.....	28
2. Graph of % Cytolysis in Nb2 Lymphoma Cells Treated with DMSO, Dex $\pm$ Prl and Prl Alone Measured by Trypan Blue.....	30
3. Photomicrograph of TUNEL Staining at 20X Objective Magnification of Nb2 Lymphoma Cells Treated With Dex for 24 Hours.....	32
4. Photomicrograph of TUNEL Staining at 40X Objective Magnification of Nb2 Lymphoma Cells Treated With Dex for 24 Hours.....	34
5. Graph of % Cytolysis in Synchronized Nb2 Lymphoma Cells Treated With DMSO and Dex Measured by Trypan Blue Exclusion.....	37
6. Graph of % Cytolysis in Synchronized Nb2 Lymphoma Cells Treated With DMSO and Dex Measured by TUNEL Assay.....	39
7. Photomicrographs of TUNEL Staining in Synchronized Nb2 Lymphoma Cells Treated With Dex and DMSO.....	40
8. Photomicrographs of TUNEL Staining of Nb2 Lymphoma Cells Treated with DMSO, Dex $\pm$ Prl and Prl for Both 2 and 8 Hours.....	43
9. Photomicrographs of GR Antibody Staining and Absorption.....	47
10. Photomicrographs of STAT5b Antibody Staining and Absorption.....	49
11. Photomicrographs of NFkB Antibody Staining and Absorption.....	51
12. Photomicrographs of Ikb $\alpha$ Antibody Staining and Absorption.....	53

## LIST OF ABBREVIATIONS

C°	Celcius
DAB	Diaminobenzidine
Dex	Dexamethasone
ddH <sub>2</sub> O	Double Distilled Water
DMSO	Dimethylsulfoxide
DNA	DeoxyRiboNucleic Acid
FCS	Fetal Calf Serum
FM	Fischer's Medium
FMM	Fischer's Maintenance Medium
GR	Glucocorticoid Receptor
GR-CFP	Glucocorticoid Receptor-Green
	Flourescent Protein Fusion
GRE	Glucocorticoid Response Element
H <sub>2</sub> O	Water
HS	Horse Serum
ICC	Immunocytochemistry
IL-1	Interleukin 1
IL-2	Interleukin 2
IL-7	Interleukin 7
ISNT	<i>In Situ</i> Nick Translation
JAK2	Janus Associated Kinase
M	Molar
ug	Micro Gram
ul	Micro Liter
mL	Mili Liter
mM	Mili Molar
ng	Nano Gram
nM	Nano Molar
Prl	Prolactin
RNA	Ribonucleic Acid
SE	Standard Error
SM	Synthetic Medium
SH2	SRC Homology 2
STAT	Signal Transducer and Activator of Transcription
Tdt	Terminal Deoxynucleotidyl Transferase
TNF	Tumor Necrosis Factor
TUNEL	Tdt-Dependent dUTP-biotin Nick End Labeling
U	Unit

## **Immunocytochemical Study of Apoptosis Signaling In Nb2 Lymphoma Cells**

### **ABSTRACT**

A thesis submitted in partial fulfillment of the requirements for the degree of Masters in Science at Virginia Commonwealth University.

Angelo Guanzon

Virginia Commonwealth University, 1998

Director: Raphael J. Witorsch, Ph.D, Professor, Department of Physiology

In the absence of mitogen, administration of Dexamethasone (Dex) induces apoptosis, or programmed-cell death in the Nb2 lymphoma cell. Addition of prolactin (Prl), on the other hand, blocks this effect. As a model for apoptosis, we were able to investigate this Dex-Prl interaction by means of a morphological approach: one that could be visualized under a light microscope. This approach allowed us to achieve several aims. First, we were able to develop a method of cell quantification befitting a morphological study based upon the hemacytometer. Second, with Trypan Blue exclusion, we were able to verify Dex/Prl-responsiveness in the Nb2 cells. Third, we were able to refine and characterize the TUNEL (Tdt-dependent dUTP-biotin Nick End Labeling) assay as a means of detecting apoptosis in both log phase and synchronized cells. With the

synchronized cells, we observed that the time frame of apoptosis onset as measured by Trypan Blue and the TUNEL assay, occurred between 6 and 8 hours. Fourth, using immunocytochemistry (ICC), we were able to characterize and establish specificity of affinity purified polyclonal rabbit antibodies directed against the signal proteins, glucocorticoid receptor (GR), STAT5b, NFkB and I $\kappa$ B $\alpha$ . Fifth, we were able to examine how these signal proteins changed in response to Dex treatment using ICC. According to our results, the percentage of positively stained cells for each of these signal proteins remained constant for each time point and treatment.

## Chapter 1

### INTRODUCTION

#### 1.1 Background

Apoptosis is a well-coordinated process of cellular suicide induced by the presence or absence of specific intracellular signals (Gerschenson et al., 1992). The Greek term “apoptosis,” which means “falling off,” was first coined by Karr and Searle in 1972, to describe programmed cell death (Karr et al., 1972). This term likens the process of cell death to the simple event of “petals falling off of a flower (Karr et al., 1972).”

Based upon this comparison, apoptosis is viewed through a naturalistic paradigm--- just as petals are seasonally shed from flowers after [having served their purposes during] fertilization, so too are cells shed from living tissues to accommodate for the growth of new cells and the restructuring of tissues (Gavrieli et al., 1992). Therefore, apoptosis is necessary in the deletion of cells during development as can be seen in embryogenesis (Wyllie, 1981; Umansky, 1982; Arends et al., 1989; Bursch et al., 1990; Ucker, 1991; Gavrieli et al., 1992), cytotoxic T-lymphocyte action (Russel et al., 1981; Duval et al., 1986; Wyllie, 1987; Arends et al., 1989) and auto-reactive T

and B-lymphocyte deletion (Shi et al., 1989; Smith et al., 1989; Arends et al., 1989). Although apoptosis is responsible for massive cell loss, it causes no permanent detriment to the natural cellular environment (Gerschenson et al., 1992). This maintenance of the natural environment is supported by the absence of any marked inflammation during apoptosis (Gerschenson et al., 1992).

The morphological and biological changes that occur during apoptosis may account for the preservation of cellular environmental stability. These changes follow a sequence of specific events as described by Wyllie (Wyllie et al., 1980). First, the cell decreases in volume due to active loss of intracellular fluid. As a result, cellular organelles become compacted as the cell increases in density. The cell surface adopts a bleb-like appearance after the endoplasmic reticulum becomes swollen and fuses with the cytoplasmic membrane. Simultaneously, the chromatin takes on a granular appearance after condensing and undergoing extensive double stranded degradation. In the latter stages, the nucleus becomes highly convoluted and the cell finally fragments into membrane bound vesicles referred to as apoptotic bodies. These bodies envelop nuclear and cytoplasmic remnants as well as intact cellular organelles. Lastly, scavenger cells phagocytize these apoptotic bodies. In essence, the cells shrink, and are cleared by phagocytes leaving behind no remnants to poison the local environment (Gerschenson et al., 1992).

The biochemical hallmark of apoptosis is DNA fragmentation or double-stranded cleavage of DNA at internucleosomal linker regions (Kerr et al., 1972). This cleavage pattern occurs as a function of the molecular structure of chromatin. The DNA double helix is wrapped twice (180 base pairs) around a nucleosomal core comprised of an octamer of histone proteins H2A, H2B, H3 and H4. Adjacent cores are connected together by short linker strands of DNA in histone H1 (McGhee et al., 1980). Cleavage by  $\text{Ca}^{2+}$  and  $\text{Mg}^{2+}$  dependent endonucleases (Gerschenson et al., 1992) at these susceptible linker regions releases the double stranded DNA fragments (Telford et al., 1989). The resulting DNA fragments are about 180 base pairs in length or multiples thereof (Gerschenson et al., 1992). These fragments can be visualized as a laddering pattern by agarose gel electrophoresis (Kerr et al., 1972; Gorczyca et al., 1993).

DNA fragmentation is an early event that commits a cell to death (Wyllie et al., 1980). However, before fragmentation occurs, transcription of various protein signals is necessary to induce apoptosis. Earlier studies involving inhibitors of transcription and translation have been shown to prevent apoptosis (Wyllie et al., 1980). Therefore, synthesis of the intracellular signals responsible for the induction of apoptosis must logically proceed DNA fragmentation. Once the cell's genome is disrupted by fragmentation, gene transcription and the protein-translation cascade that follow can no longer occur. Hence, after fragmentation of the cell's genome occurs, the cell becomes irreversibly committed to apoptosis.

Necrosis, on the other hand, is the alternative form of cell death resulting from irreversible injury or trauma (Walker et al., 1988). As a non-specific and energy independent type of death, necrosis is characterized by disrupted osmoregulation, sequential dissolution of cytoplasm and nucleoplasm, breaching of the plasma membrane, organelle deterioration, expansion and dissolution of the nucleus, increased cell volume and random single and double stranded DNA breaks (Gerschenson et al., 1992; Schwartzman et al., 1993). These random DNA breaks are visualized as smears on agarose electrophoretic gels (Gerschenson et al., 1992). Although both apoptosis and necrosis ultimately result in cell death, these phenomena require different stimuli and signals for their induction. While trauma such as ischemia, exposure to extreme temperatures and pHs and direct cell injury are known to induce necrosis, the signals which invoke apoptosis are involved in a much more complex interaction (Walker et al., 1988). In this study, we will be instituting an immunocytochemical and morphological approach in examining some of these intracellular signals involved in the induction and modulation of apoptosis.

Previous work in our laboratory used the Nb2 lymphoma cell as a model to study control of apoptosis. The Nb2 lymphoma is an early T-cell thymocyte originating from a male Nobel rat treated with estrogen (Gout et al., 1986) possessing both CD4 and CD8 surface cell markers (Fleming et al, 1982). The morphology of the Nb2 lymphoma cell, typical of a neoplastic cell, exhibits a high nucleus to cytoplasmic ratio. Characteristically, each cell contains a large horseshoe-shaped nucleus



accompanied by a prominent nucleolus, all of which are surrounded by scanty amounts of cytoplasm (Fleming et al., 1982). The cytoplasm contains a multitude of polyribosomes and numerous mitochondria (Fleming et al., 1982). Nb2 lymphoma cells, under stationary conditions, average about 7.5  $\mu\text{m}$  in diameter, and 9  $\mu\text{m}$  during logarithmic growth conditions (Fleming et al., 1982).

Sensitive to lactogenic hormones for proliferation, Nb2 cells require about 1 ng/ml prolactin (Prl) for robust growth (Gout et al., 1986); a dose that is less than circulating physiological Prl concentrations (Tanaka et al., 1980). Therefore, supplementing stationary media or Fischers Media (FM) with lactogenic hormones such as Prl, fetal calf serum (FCS), interleukin-2 (IL-1) and interleukin-7 (IL-7) induces Nb2 cell propagation in culture (Murphy et al., 1988, Sadeghi et al., 1992; La Voie et al., 1994).

It has been shown that glucocorticoids promote cytolysis in lymphocytes (Compton, 1986). Earlier work done in our laboratory reveals that treatment of Nb2 cells with the synthetic glucocorticoid dexamethasone (Dex) induces apoptosis in a receptor-mediated and dose-dependent manner (Fletcher-Chiappini et al., 1993). Moreover, it was discovered that Dex inhibits the mitogenic effect of Prl in Nb2 cells in a dose-dependent fashion (Fletcher-Chiappini et al., 1993). On the other hand, further investigation shows that Prl inhibits Dex-induced apoptosis in the same cell line

(Fletcher-Chiappini et al., 1993). This interaction between Dex and Prl seen in the Nb2 cell provides a dynamic model for our investigation of apoptosis control.

Previous investigation of apoptosis focused on biochemical and molecular biological approaches. Techniques such as the diphenylamine assay, DNA fragmentation assay/agarose gel electrophoresis, Western blot analysis, RNA synthesis inhibition assays and protein synthesis inhibition assays were instrumental in exploring key elements involved in programmed cell death (Gerschenson et al., 1992). Despite these advancements, biochemical and microbiological approaches provide only partial insight into the grand scheme of apoptosis. Because biochemical techniques do not preserve structural integrity of the cells, qualitative information that may be gathered from cell morphology, may be lost. Furthermore, techniques such as the diphenylamine assay and DNA fragmentation/agarose gel electrophoresis can only provide quantifiable data from a relatively large threshold number of cells. Typically, between  $0.5 \times 10^6$  and  $2 \times 10^6$  cells are used to generate DNA fragmentation bands for agarose gel electrophoresis (Compton et al., 1986; La Voie et al., 1995). Any physiological changes or effects seen in only a few of the cells in the population are diluted out when the cells are homogenized and analyzed with biochemical assays. Gavrieli states in support of this idea, "The drawback [of DNA fragmentation], however, is that the procedure uses involved homogenization of the entire cell population and an analysis of the pooled DNA extract (Gavrieli et al., 1992)." Both

quantitative and qualitative data from individual cells cannot be collected by these techniques.

To furnish greater insight into this phenomenon, we have adopted a morphological and immunocytochemical approach in our study of programmed cell death. This approach would appear to offer several advantages over disrupted cell methods. First, morphological techniques such as immunocytochemistry (ICC) and the Tdt-dependent dUTP-biotin Nick End Labeling (TUNEL) assay preserve the cell's structural integrity allowing the morphological and cytological features of a cell to be viewed. This preservation occurs as a function of the mild preparations and fixatives involved in these cytological assays. In doing so, qualitative information about the "ultrastructural process" of apoptosis may be ascertained from an intact cell at different time points and under different magnifications (Gavrieli et al., 1992, Tornusciolo et al., 1995).

Second, a morphological study not only allows for the visualization and quantification of groups of cells, but also allows for the visualization of apoptosis at the individual cell level under the light microscope (Gavrieli et al., 1992). Thus, cell number would appear not to be a limiting factor with this methodology.

Third, this approach can be modified from a single immunological staining protocol to a multiple immunological staining protocol in order to co-localize various intracellular signals using multiple antibodies in the same assay. Furthermore, the

TUNEL assay can be used in concert with the ICC assay to visualize whether cells in a population undergoing apoptosis are the same cells that stain positive for a particular signal protein. Tornusciolo states, “An immunohistochemical multi-labeling technique would be one means of simultaneously identifying apoptotic cells, [and] determining their immunophenotype (Tornusciolo et al., 1995).”

Fourth, according to Gavrieli, staining of apoptotic cells using the morphological technique, the TUNEL assay, has been shown to “precede (and, therefore, does not depend on) the appearance of the nucleosomal ladder” found in DNA fragmentation/agarose gel electrophoresis (Gavrieli et al., 1992). Using thymocytes, Gavrieli demonstrated that the TUNEL assay can detect Dex-induced apoptosis as early as 1.5 hours whereas DNA fragmentation/gel electrophoresis can detect laddering only after 3 hours (Gavrieli et al., 1992). Thus, in theory, the TUNEL assay may be a more effective method of detecting apoptosis, especially at earlier time points.

The TUNEL assay was developed in 1992 by Gavrieli, as an immunological assay for specifically detecting apoptosis (Gavrieli et al., 1992). This particular system works by labeling double-stranded breaks in internucleosomal regions of genomic DNA. As was indicated earlier, DNA fragmentation is a signature characteristic of cells undergoing apoptosis. The enzyme Terminal Deoxynucleotidyl Transferase (Tdt) targets, then covalently incorporates biotinylated nucleotides to the ends of these

DNA fragments. The biotinylated nucleotides are detected using a Streptavidin-Horseradish Peroxidase conjugate that binds to biotin. Streptavidin-Horseradish Peroxidase then enzymatically cleaves the soluble and colorless chromophore Diaminobenzidine (DAB) generating an insoluble and colored substrate marking where DNA fragmentation has occurred (Trevigen, Inc., 1996; Gavrieli et al., 1992). With the TUNEL assay one is not only able to determine which cells in the population are undergoing apoptosis, but also can visualize actual cellular morphology of cells undergoing apoptosis under the light microscope. We selected the TUNEL assay instead of the *In Situ* Nick Translation (ISNT) assay which uses DNA Polymerase I enzyme to label DNA when one strand is nicked (Gold et al., 1994). Reports by Gold indicate that the TUNEL assay is more sensitive and specific than the ISNT assay for detecting apoptosis (Gold et al., 1994).

Through the use of ICC, we are able to examine both the signal proteins associated with control of apoptosis and the changes in these signals preceding apoptosis. Affinity purified polyclonal rabbit antibodies and antibody absorption has allowed us to establish and characterize the presence and specificity of the proteins GR, STAT5b, NF $\kappa$ B and I $\kappa$ B $\alpha$  in the Nb2 lymphoma cell. These proteins have been implicated as intracellular signals involved in the apoptotic pathway. In order to establish a greater understanding of the apoptotic involvement of these signals, the characteristics and modes of action of each protein of interest should be discussed.

As a ligand-regulated transcription factor, the glucocorticoid receptor (GR) is the signal associated with the Dex response; GR controls genes necessary for the initiation of glucocorticoid-induced thymocyte apoptosis (Flomerfelt et al., 1994). GR exists in two isoforms,  $\alpha$  and  $\beta$ , which are 95 and 90 kDa in length respectively (Vedeckis, 1992, Santa Cruz Biotechnology, Inc., 1997).  $\alpha$ GR is the most abundant isoform. In unstimulated cells, GR is localized predominantly in the cell cytoplasm (Antakly et al., 1989).

The structure of GR consists of a nonconserved amino terminus followed by a highly conserved DNA-binding domain (Vedeckis, 1992). The DNA-binding domain is comprised of two cysteine zinc fingers that bind to the response element on DNA (Vedeckis, 1992). A nonconserved hinge region connects the DNA-binding domain to the conserved ligand-binding domain at the carboxyl terminus (Vedeckis, 1992). The mechanism of GR action, similar to other steroid hormone receptors, occurs in the following manner. After the glucocorticoid ligand binds to the carboxyl terminus of the receptor, the cytosolic receptor translocates to the nucleus (Picard et al., 1987, Wilkstrom et al., 1987, Antakly et al., 1989). In the nucleus, the receptor protein then binds to its cognate, specific DNA response element to regulate gene transcription (Vedeckis, 1992).

STAT5b protein is a member of a family of signal transducers and activators of transcription (Stocklin et al., 1996). It has been implicated as a protein modulator

involved in the Prl signaling cascade (Stout et al., 1996). Sharing homology with other STAT proteins, STAT5b possesses the following domains: (1) an amino terminus helical domain possibly involved in protein/protein interactions, (2) a helix-B pleated sheet-helix domain necessary for binding DNA, (3) an SRC homology 2 (SH2) domain necessary for STAT/STAT and STAT/receptor interactions through phosphorylated tyrosines, (4) a tyrosine residue crucial for STAT/STAT intermolecular interaction, nuclear translocation and transactivation at the carboxyl terminus (Yu-Lee, 1997). In the absence of Prl stimulation, STAT5 is localized primarily in the cell cytoplasm (Stout et al., 1997).

The mode of action involved in the Prl/STAT5b signaling pathway occurs in the following manner as described by Yu-Lee (Yu-Lee, 1997). After Prl binds to Prl receptors (Prl-R), the receptors dimerize. Dimerization activates Prl-R associated Janus Associated Kinase 2 (JAK2) which then phosphorylates the Prl-R intracytoplasmic domain (on tyrosine). STAT5b then docks onto the phosphorylated tyrosine on the intracytoplasmic domain via its SH2 domain. JAK2 is then able to phosphorylate tyrosine residues on STAT5b. Phosphorylated STAT5bs become activated and form homo- or heterodimers via their SH2 domains. These dimers then translocate to the nucleus and bind corresponding DNA response elements to modulate gene transcription (Yu-Lee, 1997). According to Stout, nuclear translocation of STAT5 can be seen via immunocytochemistry after 1 hour of Prl treatment (Stout et al., 1997). Hence, in the case of the Nb2 cell, binding of Prl to its

receptor follows the Prl-R/STAT5b cascade eventually leading to cell proliferation (Camarillo et al., 1996).

As was stated earlier, an antagonistic interactive relationship exists between Dex and Prl in the Nb2 cell. Dex inhibits Prl-induced mitogenesis, while Prl prevents Dex-induced apoptosis. At the present time, the mechanism behind this interaction is unknown. However, several theories may attempt to explain this phenomenon. Prl may inhibit Dex-induced apoptosis by interaction with GR. First, Prl action may down regulate GR in the cytoplasm preventing ligand-receptor binding. Second, Prl may interfere with GR nuclear translocation or impede GR binding to GR response elements on chromatin. However, these two cases are not likely candidates because Dex, functioning by way of GR, is known to cause inhibition of Prl-induced mitogenesis. Hence, in order to activate this response, GR must be functional in order to bind its ligand, to translocate to the nucleus and to bind its cognate response element. Third, Prl may prevent downstream GR-induced post-transcriptional or translational events responsible for apoptosis, from occurring.

From the other perspective, Dex may inhibit Prl-induced mitogenesis by GR interaction with Prl associated signal pathways. GR may interact and inhibit the action of signals such as STAT1, 3, 5a and 5b, Fyn, Raf and Src which have been implicated in the Prl signaling pathway in Nb2 cells (Yu-Lee, 1997). While GR may interfere with these Prl signals mediating mitogenesis, other Prl signals mediating



anti-apoptosis may operate without impairment. It is also unlikely that Dex interferes with Prl receptor actions since the latter exhibits anti-apoptotic actions under these conditions.

As one possible model, Stocklin et al. (1996) suggests that a functional interaction exists between GR and STAT5b in mammary epithelial cells that may account for the inhibitory effect of Prl on Dex-induced apoptosis in lymphocytes. In effect, STAT5 forms a complex with GR, binding to DNA in a manner independent of the glucocorticoid response element (GRE) (Stocklin et al., 1996). This GR/STAT5 interaction may diminish the response by glucocorticoids at the GRE-promotor, thereby inhibiting apoptosis (Stocklin et al., 1996). At the same time, the GR/STAT5 complex may upregulate STAT5-response element-containing promoters and accordingly, the STAT5 response as occurs in mammary epithelial tissue (Stocklin et al., 1996). Therefore, the inhibition of glucocorticoid-induced apoptosis of lymphocytes may be a function of the Stat-mediated suppression of gene induction by GR (La-Voie et al., 1995, Stocklin et al., 1996). Studies by Fletcher-Chiappini show the opposite side of the Dex/Prl interaction, in which Dex blocks the mitogenic effect of Prl on Nb2 cells (Fletcher-Chiappini et al., 1993). This Dex/Prl interaction seems to counter Stocklin's assertion that GR/STAT5 complex upregulates STAT5 response (ie. proliferation in Nb2 cells). Despite this STAT5 upregulation, the apoptotic effects of Dex may balance the mitogenic effects of STAT5 resulting neither in mitogenesis nor apoptosis.

NFκB or nuclear factor kappa B, is a protein transcription factor reported to be an inhibitor of apoptosis. Activated by such pro-inflammatory cytokines as interleukin-1 (IL-1) and Tumor Necrosis Factor (TNF), NFκB turns on cell genes in response to inflammation, stress and infection (Barinaga, 1996). The most common form of NFκB exists as a heterodimer comprised of a 50-kD protein (p50) and a 65-kD protein (p65) (Beg et al., 1996). NFκB on the other hand, is inhibited in an antagonistic interplay with the cytoplasmic repressor protein IκBα. As a 37-kD protein, IκBα contains a series of ankyrin-like repeat motifs that interact with NFκB and prevent its translocation into the nucleus (Israel, 1995).

The interaction between NFκB and IκBα occurs by the following mechanism. In unstimulated cells, NFκB is complexed with IκBα in the cytoplasm preventing its translocation into the nucleus. Stimulation of the cells results in the phosphorylation of IκBα at conserved amino acid residues Ser32 and Ser36 by various kinases (Brown et al., 1995). Studies have suggested these kinases to be protein kinase C-δ and Raf protein kinase acting in concert with p-68-protein kinase (Israel, 1995).

Phosphorylation of IκBα results in its proteolytic degradation, releasing NFκB from inhibition (Brown et al., 1995). It is still under speculation as to whether IκBα is degraded before or after it has dissociated from NFκB (Israel, 1995). Liberated NFκB then translocates to the nucleus where it binds to its respective response element and activates gene transcription (Brown et al., 1995).

The interaction between GR and NF $\kappa$ B /I $\kappa$ B $\alpha$  can be seen in the immunosuppressive and anti-inflammatory actions of glucocorticoids (Auphan et al., 1995).

Glucocorticoids, functioning by way of the GR, have been shown to promote apoptosis in thymocytes by inducing transcriptional activation of I $\kappa$ B $\alpha$  (Scheinman et al., 1995). Studies performed by Scheinman reveal that activated GR translocates to the nucleus, binds to its DNA response element and directly induces transcription of I $\kappa$ B $\alpha$  (Scheinman et al., 1995). As a result, more I $\kappa$ B $\alpha$  protein becomes available to bind and inhibit the anti-apoptotic actions of NF $\kappa$ B (Auphan et al., 1995). In fact, increased production of I $\kappa$ B $\alpha$  by glucocorticoids have been shown to sequester DNA-bound NF $\kappa$ B from the nucleus back into the cytoplasm (Auphan et al., 1995). As a consequence of the increased inhibition of NF $\kappa$ B, lymphocytes involved in the immune response are more susceptible to apoptosis (Auphan et al., 1995).

Another feature examined via ICC and light microscopy is the localization of these signal proteins of interest within the Nb2 cell following different treatment conditions (i.e. Dex and DMSO). Such a study focuses on the location of staining within the cell. Staining localized in the nucleus suggests nuclear translocation of the protein while peripheral staining suggests cytoplasmic localization. Using this methodology, we questioned whether it was possible to visualize nuclear staining.

In the past, nuclear translocation of intracellular signals had been examined by various methodologies. In fact, nuclear translocation of GR has been well

documented using techniques such as electrophoretic mobility-shift assays (Tanaka et al., 1992), radiolabeling of homogenized cells (Kaufmann, et al., 1982) and immunoprecipitation assays (Tanaka et al., 1996). While these techniques involved examination and quantification of GR protein in disrupted cells, few of these studies actually provided a visual representation of GR nuclear translocation. However, work by Carey, utilized direct fluorescence microscopy and glucocorticoid receptor-green fluorescent protein fusion (GR-GFP) to demonstrate real-time imaging of GR nuclear transport (Carey et al., 1996). Along the same lines, studies performed by Antakly et al. (1989) actually implemented light microscopy to view GR nuclear translocation. Electronmicroscopy was used to confirm that nuclear translocation did indeed occur (Antakly et al., 1989). Although these studies did not quantify the percentages of cells exhibiting nuclear translocation, these studies demonstrated that nuclear translocation could be viewed with light microscopy.

## 1.2 Purpose of Study

The main purpose of our study is to test the feasibility of the morphological approach in the investigation of apoptotic control in Nb2 lymphoma cells. In order to establish this criteria, we refined and characterized the TUNEL assay as a means of detecting apoptosis and its kinetics in Nb2 cells. Next, using ICC, we demonstrated that the intracellular signal proteins GR, STAT5b, NFkB and Ikb $\alpha$  exist in Nb2 cells by way of affinity purified rabbit polyclonal antibodies and immunoperoxidase staining. In

doing so, we also established specificity of this immunostaining by absorption of the antibodies with corresponding peptides. Lastly, with ICC, we determined whether it is possible to visually detect changes in the appearance, localization and intensities of these signals in Nb2 cells undergoing apoptosis.

## Chapter 2

### MATERIALS AND METHODS

#### 2.1 Maintenance of Nb2 Lymphoma Cells

Wild-type Nb2 cells (Nb2-U17) were provided by Dr. Robert Adler of the McGuire Veterans Hospital. Dr. Peter Gout of the Cancer Control Agency of British Columbia was the original provider of the cells. Cells stored as frozen aliquots (-70°C) were resurrected and maintained as previously reported in Fischer's Maintenance Medium (FMM) which consists of Fischer's medium (FM) for leukemic cells of mice fortified with 10% fetal calf serum (FCS), 10% horse serum (HS), 50U/ml penicillin, 50ug/ml streptomycin, 0.1mM B-mercaptoethanol and 0.075% NaHCO<sub>3</sub> (Tanaka et al., 1980). Cell cultures were seeded between the concentrations of 0.5 × 10<sup>6</sup> and 1 × 10<sup>6</sup> cell/ml and passed every third day (approximately 72 hours). Cultures were incubated in a CO<sub>2</sub> incubator (humidified atmosphere of 5% CO<sub>2</sub> and 95% room air at 37°C). Cell concentration and viability were determined using a hemacytometer and Trypan Blue purchased from Gibco BRL (0.1 ml of cells in media plus 0.9 ml of Trypan Blue). Counts were performed in triplicate. Previous studies by Fletcher-Chiappini (1993)

established that triplicate cell counts provide the most time-effective method of attaining a valid estimate of cell count and viability.

## 2.2. Chronic (24 Hours) Dex Cytolytic Assay, Acute (Time Point) Dex Cytolytic Assay and Dex-Prl Co-Incubation Assay.

The protocol for these assays were adapted from procedures previously implemented in our laboratory with minor modifications (Fletcher-Chiappini et al., 1993, LaVoie et al., 1994). Cultured cells maintained in FMM (approximately  $0.5-0.75 \times 10^6$  cells/ml) were harvested then centrifuged at 1000 rpm for 5 minutes at 8-10°C. The cells were resuspended in FM, mixed then re-centrifuged. This step was repeated two more times (washing step). The cells were then reconstituted in Synthetic Media (SM). SM is comprised of FM supplemented with 0.1 mM B-mercaptoethanol, 50U/ml penicillin, 50ug/ml streptomycin, 15mM HEPES, 0.15% bovine serum albumin, 4ug/ml linoleic acid, 1mM pyruvate, 12ug/ml transferrin, 1.5ng/ml selenium, 1X vitamins, 0.33X amino acids, 100uM spermidine and 0.5mM  $\text{CaCl}_2$  at a pH of 7.4 .

Cell concentration and viability were then measured by Trypan Blue exclusion. For the chronic Dex-cytolytic assay, the final cell concentration was plated at  $0.5 \times 10^6$  cell/ml at a final volume of 1.5ml in SM. The following treatments were added to the

cells: (1) 0.125% Dimethyl Sulfoxide (DMSO) and (2) 100nM Dex. The cells were incubated for 24 hours at 37°C in a 5% CO<sub>2</sub> incubator.

For the acute Dex-cytolytic assay and the Dex-Prl co-incubation assay, cells were incubated in SM for 24 hours at 37°C in a 5%CO<sub>2</sub> incubator for synchronization. This synchronization step induces greater than 90% of the cell population to enter into the G1/G0 phase of the cell cycle (LaVoie, Ph.D. thesis). Synchronized cells have been shown to respond to Dex treatment at earlier time points than cells in logarithmic growth (Fletcher, Ph.D. thesis, LaVoie et al., 1994).

Cells were then counted for cell number and viability. The final concentration of cells were plated at  $2 \times 10^6$  cell/ml in a final volume of 3ml in SM. For the acute Dex-cytolytic assay, the following treatments were added to the cells: (1) 0.125% DMSO (2) 100nM Dex. The cells were incubated in each treatment at 37°C in a 5% CO<sub>2</sub> incubator for 0 (logarithmic growth and synchronized controls), 1, 2, 4, 6 and 8 hours. For the Dex-Prl co-incubation assay, the following treatments were added to the cells: (1) 0.125% DMSO (2) 100nM Dex (3) 100nM Dex + 1 ng/ml Prl (4) 1 ng/ml Prl. These cells were incubated for 8 hours at 37°C in a 5% CO<sub>2</sub> incubator. For all three assays, cells were harvested according to their respective incubation times for both hemacytometer counts and formaldehyde fixation.



## 2.3 Cell Fixation

Approximately  $3 \times 10^6$  cells were harvested from the assay plate and centrifuged at 1000 rpm for 5 minutes in an Eppendorff microcentrifuge. The cells were resuspended in 3.7% Formaldehyde (Fischer Brand) in 0.01M PBS (original pH 7.1) and allowed to incubate for 10 minutes at room temperature. After re-centrifugation, the fixative was removed and the cells were reconstituted in 0.01M PBS. The fixed cells were then spotted onto pre-etched circles (approximately 5mm in diameter) on Fischer Brand Super Frost Plus microscope slides and allowed to dry at room temperature. Each etched circle on the slide contained approximately 60,000 cells. Earlier pilot experiments showed that the use of Superfrost Slides (recommended by Trevigen) and formaldehyde fixative (recommended by Dr. Steven Grant of the Medical College of Virginia) facilitated cell adhesion.

## 2.4 TUNEL (Tdt-dependent dUTP-biotin Nick End Labeling) Assay

The TUNEL assay kit was purchased from Trevigen Inc., Maryland. The following protocol was used with minor modifications from the original Trevigen protocol: Fixed cells spotted onto Fischer brand Superfrost slides (as described above) were hydrated in 0.01M PBS for 10 minutes at room temperature. Cells were then permeabilized in Cytopore detergent for 20 minutes at room temperature. The cells were washed with 0.01M PBS (pH 7.1) in between individual steps. Exogenous

peroxidase activity was then quenched with 2% H<sub>2</sub>O<sub>2</sub> in double distilled H<sub>2</sub>O (dd H<sub>2</sub>O) for 5 minutes at room temperature. The cells then equilibrated in 1X Labeling buffer.

Next, the Tdt labeling mixture was prepared by adding 1ul of Tdt dNTP mix, 1ul of 50X Co<sup>2+</sup> and 1ul of Tdt for every 50ul of 1X Labeling mix. Tdt labeling mixture was added to each circle and allowed to incubate at 37°C for 1 hour. Afterwards, the slides were immersed in 1X Stop Buffer at room temperature for 5 minutes.

Streptavidin-Horseradish Peroxidase in 0.01M PBS was added and allowed to incubate at room temperature for 10 minutes. The slides were then bathed in DAB solution consisting of 50ml of 0.01M PBS, 250ul of DAB stock solution and 50ul of 30% hydrogen peroxide for 10 minutes at room temperature. The slides were stored in ddH<sub>2</sub>O. Next, slides were dehydrated by sequential exposure to 50% ethanol, 70% ethanol, 95% ethanol, 100% ethanol and xylene and coverslipped with Protex mounting medium.

## 2.5 Immunocytochemistry

Affinity purified polyclonal rabbit antibodies directed against the cellular proteins and respective antigens glucocorticoid receptor (P-20), STAT5b (C-17), IκBα (C-21) and NFκB (C-20) were purchased from Santa Cruz Biotechnology at the initial concentration of 100ug/ml to 200ug/ml. The antibodies were then diluted to obtain

the working concentration of 2 $\mu$ g/ml in 0.01M PBS/0.1% BSA. GR antibody reacts with a peptide corresponding to amino acids 750-769 mapping at the carboxyl terminus of glucocorticoid receptor  $\alpha$  of human origin. This antibody is non-cross reactive with GR $\beta$ . STAT5b antibody interacts with a peptide corresponding to amino acids 706-722 mapping at the carboxyl terminus of STAT5b of mouse origin. This antibody reacts with both STAT5a and STAT5b. Anti-NF $\kappa$ B reacts to corresponding amino acids 531-550 mapping at the carboxyl terminus of NF $\kappa$ B p65 of human origin. Lastly, I $\kappa$ B $\alpha$  antibody is directed against a peptide corresponding to amino acids 297-317 mapping at the carboxyl terminus of I $\kappa$ B $\alpha$  of human origin. All of the above were specified as being reactive to the corresponding proteins in the rat (Santa Cruz Biotechnology Inc., 1997).

Vectastain ABC peroxidase anti-rabbit kit was used to visualize binding of these antibodies within the cells. Mixing the proper dilutions of the working concentrations of both the antibodies and the Vectastain solutions was empirically achieved. Tinctorial staining of Nb2 cells was obtained by 30-second incubations in Wright's Giemsa stain (Gibco).

The following immunocytochemical protocol was used: Fixed cells were hydrated in a 0.01M PBS for approximately 5 minutes at room temperature. Paraffin embedded pituitary slides (the method control) were deparaffinized by sequential exposure to xylene, 100% ethanol, 95% ethanol, 70% ethanol, 50% ethanol and ddH<sub>2</sub>O. The

pituitary slide was then hydrated in 0.01M PBS. At no time after hydration were the cells allowed to desiccate. Unless otherwise specified, immunoreagents were applied in drops to the specimen. Incubation was conducted in a humidified airtight container. Furthermore, slides were washed by flooding and immersion in 0.01M PBS between incubation periods.

The cells were permeablized in 0.2% Triton X-100 in 0.01M PBS for 30 minutes at room temperature. Next, the cells were bathed in blocking solution for 20 minutes at room temperature. Primary antibody was added and then allowed to incubate for 3 hours at room temperature. Canine Prl antibody was added to pituitary samples at dilutions of 1:1,600, 1:3,200, 1:6,400 and 1:12,800. Following incubation, the cells were treated with a 12.5% standard working stock dilution of Vectastain biotinylated antibody for 30 minutes at room temperature. Afterwards, the cells were exposed to a 20% standard working stock dilution of Vectastain ABC reagent in 0.01M PBS (pH 7.4) for 30 minutes at room temperature.

The slides were then immersed in DAB solution consisting of 12.5 mg DAB/50ml of 0.05M Tris HCl (pH of 7.6) containing 50ul H<sub>2</sub>O<sub>2</sub>. The slides incubated for 10 minutes at room temperature. The slides were then sequentially exposed to ddH<sub>2</sub>O, 50% ethanol, 70% ethanol, 95% ethanol, 100% ethanol and xylene and coverslipped as previously described.

## 2.6 Confirmation of Polyclonal Rabbit Antibody Specificity via Antibody

### Absorption

Specificity of polyclonal rabbit antibodies was verified by performing antibody absorption incubations with peptides specific for each antibody. Based upon the specifications provided by Santa Cruz Biotechnology, absorption should involve exposure of the antibody to 10X greater concentration of the antigen. Accordingly, for the absorption sample, 2ug of specific peptide in a volume of 10ul was added to 100ul of antibody at a concentration of 2ug/ml (0.2ug total antibody). For the negative control sample, 10ul of PBS-0.02% BSA was mixed with 100ul of antibody at a concentration of 2ug/ml. Both of these samples were incubated overnight at 4 °C. After incubation, these mixtures were applied to log phase and synchronized Nb2 cells in an ICC assay. Specificity of immunostaining was validated if absorption of antibody eliminated such staining (Witorsch, 1980).

## 2.7 Photography

Cell fields were photographed using a Nikon microscope camera with Kodak Ectachrome Elite 100 color film. To obtain representative cell samplings from the slides, photomicrographs were taken of four fields at positions analogous to 2, 4, 8 and 10 o'clock in the etched circle. These photomicrographs were taken at 20 and

40x objective magnification to obtain sufficient numbers of cells in the field. The magnifications on 35mm E-6 color slides were 10 and 20x respectively.

## 2.8 Cell Quantification

The cell images on 35mm slides were scanned with Sprint Scan onto a computer-imaging program (Corel Photo-Paint 6) and used to make four color templates of each incubation (corresponding to the fields originally photographed). These fields were then counted from photomicrographs measuring the number of total cells, number of positively stained cells and the number of cells with centralized staining. For each cell sample, the number of cells counted ranged from 400 to 1600 cells.

## 2.9 Statistics

Data from at least three individual experiments (i.e. experiments performed on different days) were used to generate means and standard errors. The different treatments were compared by analysis of variance and then by Duncan's multiple range tests (Duncan, 1955; Kramer, 1956). Statistical analysis was performed using Sigma Stat 2.0 computer software. A  $P \leq 0.05$  was the minimum acceptable level of significance.

## **Chapter 3**

### **RESULTS**

#### **3.1 Morphology of Nb2 Lymphoma Cells**

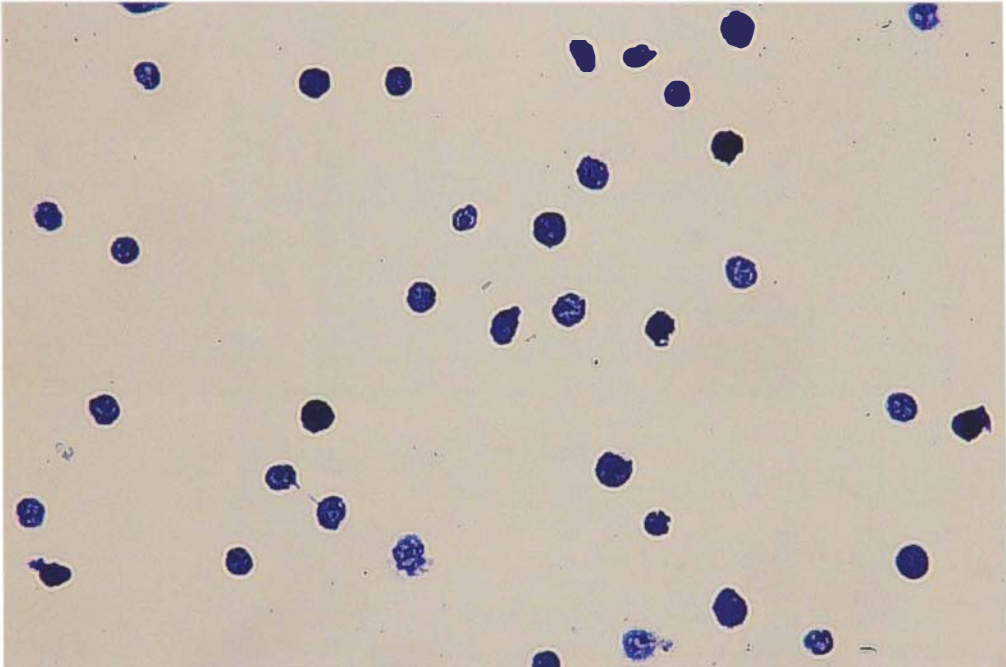
Figure 1 shows Nb2 cells stained with Wright's Giemsa stain. As can be seen, the morphology of the Nb2 cell is typical of a neoplastic lymphoma cell exhibiting a high nucleus to cytoplasm ratio (Fleming, et al., 1982).

#### **3.2 Hormone Responsiveness to Dex $\pm$ Prl Treatment of Log Phase Nb2 Cells as Measured By Trypan Blue Exclusion and the TUNEL Assay.**

Trypan Blue exclusion counts of non-synchronized Nb2 cells treated with Dex  $\pm$  Prl for 24 hours serve to confirm earlier reports (Fletcher-Chiappini et al., 1993). Figure 2 indicates that 100nM Dex produces a significant 2.75-fold increase in the percentage of dead cells above DMSO control ( $P \leq 0.05$ ,  $n=3$ ). Co-incubation of Dex with Prl at 1 ng/ml blocks this effect.

Figure 1. Nb2 lymphoma cells at 354x magnification stained with Giemsa stain. The Nb2 cell exhibits morphology typical of a neoplastic lymphoma cell.





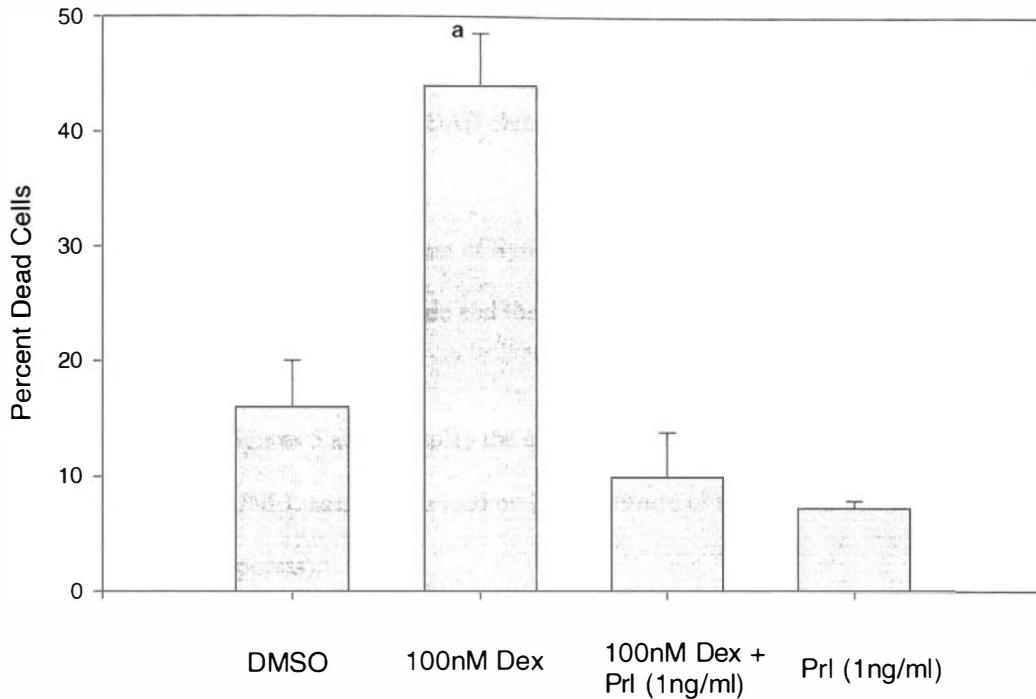


Fig. 2. Trypan Blue Exclusion counts performed on 24 Hour Dex and Prl co-incubation experiments in Nb2 Lymphoma cells show significant changes ( $P \leq 0.05$  and  $n=3$ ) between treatments as indicated by the superscript (a). Dex treatment produces a significant 2.75-fold increase in the percentage of dead cells above the DMSO control. Co-incubation of Dex with Prl (1ng/ml) blocks this effect. Prl treatment and 100nM Dex + Prl treatment both reveal no significant change from DMSO control.

<sup>a</sup>significantly different at  $P < 0.05$  vs DMSO control, Dex + Prl treatment and Prl treatment alone

As shown in Figures 3 and 4, Dex exposure for 24 hours produces a marked increase in the TUNEL labeling of log phase Nb2 cells. At higher magnification (Figure 4 at 40X objective magnification), the fragmented nuclei containing dense chromatin, a typical morphological feature of apoptosis, can be seen. The chromatin are clearly stained and outlined by the DAB chromophore.

### 3.3 Hormone Responsiveness of Synchronized Nb2 cells to Dex $\pm$ Prl Treatment as Measured by Trypan Blue and the TUNEL Assay.

Table 1, Figures 5 and 6 display the quantified data from both Trypan Blue exclusion and the TUNEL assay performed on Dex exposure of synchronized Nb2 cells (0-8 hour time points).

Trypan Blue exclusion counts demonstrate that cytolysis is first evident after 6 hours of Dex incubation, and even more so after 8 hours. In both the 6 and 8-hour time points, data indicates a significant increase in the number of dead cells relative to DMSO control (Table 1, Figure 5 at  $P \leq 0.05$ ). Although not statistically significant, an increase in the percentage of basal death is seen in the 1, 2, 4, 6 and 8-hour time points when compared to cell populations in logarithmic growth and 0 hour synchrony.

Figure 3. A displays a TUNEL assay at 177x magnification performed on Nb2 cells treated with DMSO for 24 hours. B shows the increase in TUNEL staining of Nb2 cells treated with 100nM Dex for 24 hours.

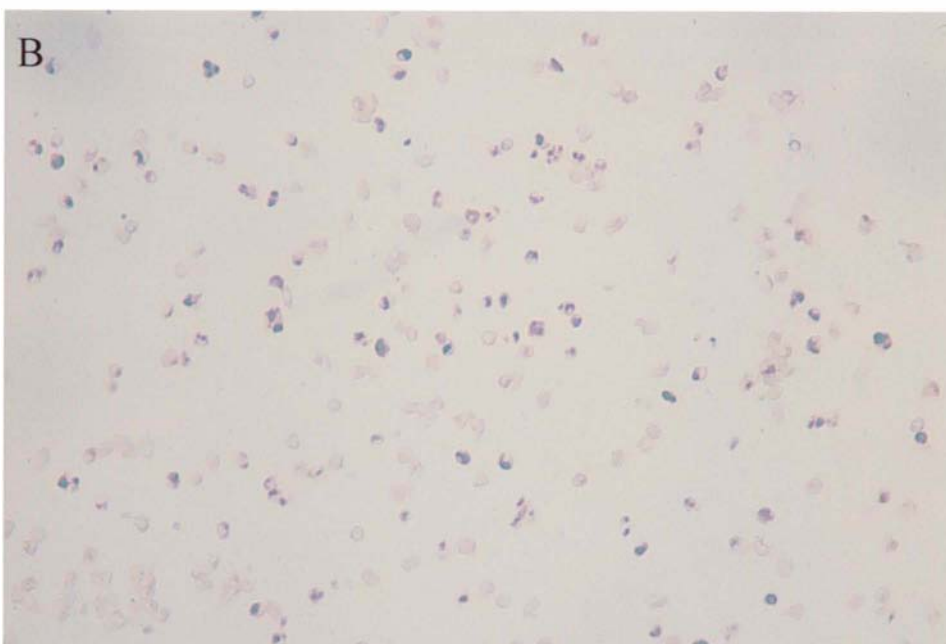
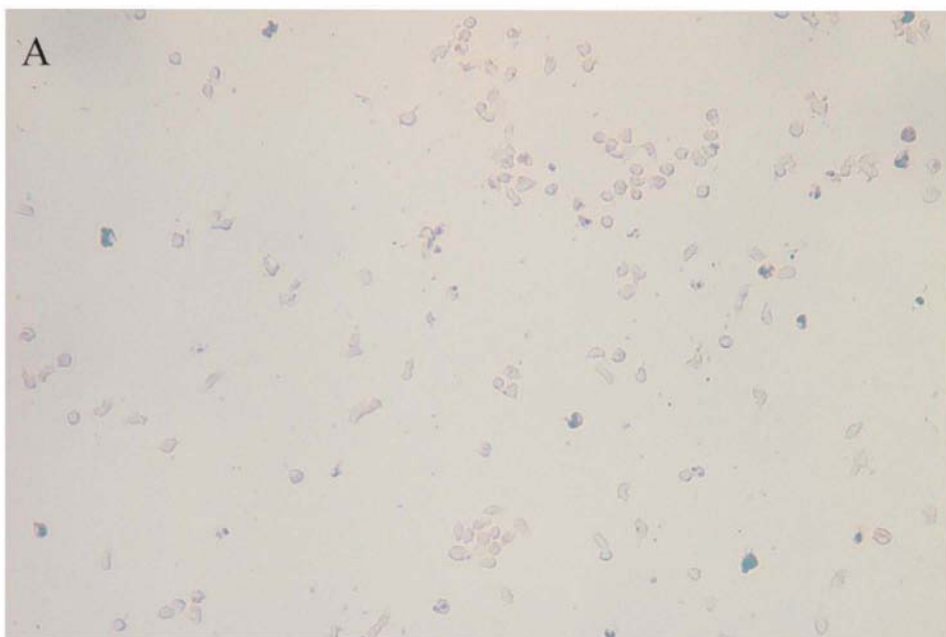


Figure 4. A exhibits a TUNEL assay performed on Nb2 cells treated with DMSO for 24 hours at 354x magnification. B shows the increase in TUNEL staining of cells treated with Dex for 24 hours. This magnification displays the morphological features of an apoptotic cell. The DAB chromophore darkly stains the apoptotic vesicles within the cells.

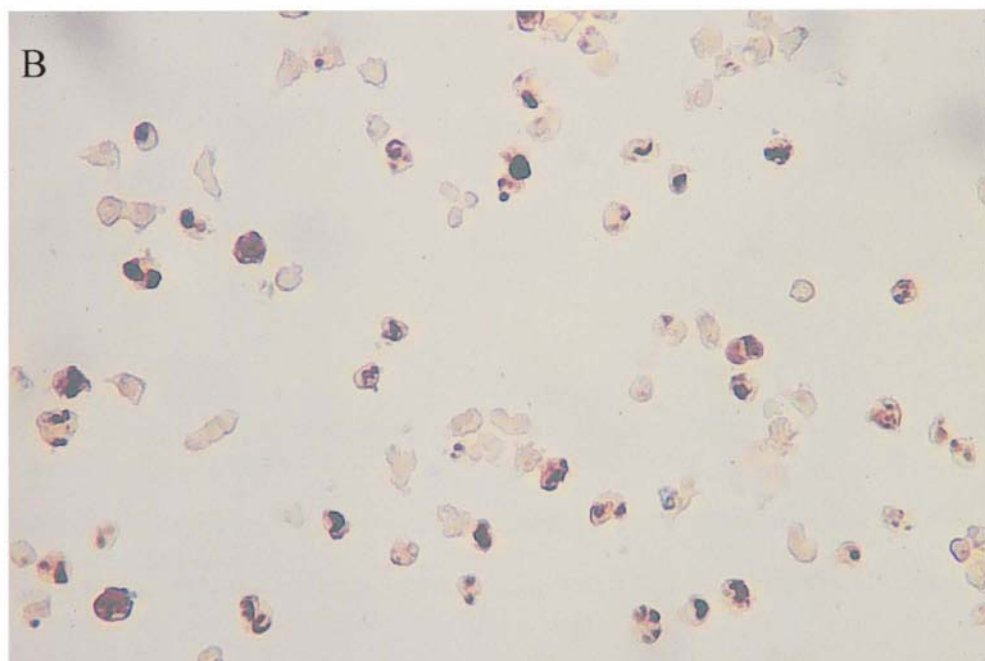
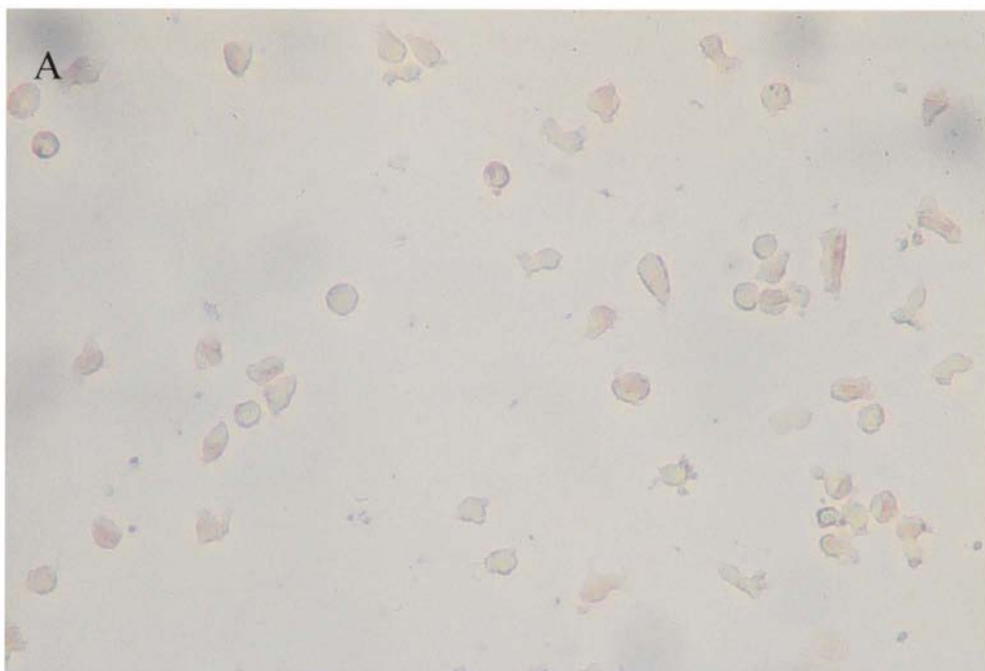


Table 1. The Effects of DMSO and Dex Treatment on Synchronized Nb2 Lymphoma Cells After 0, 1, 2, 4, 6 and 8 Hour Incubation Periods.

Time (Hours)	Treatment	Percent Dead Cells Measured By Hemacytometer/ Trypan Blue Exclusion (%)	Percent Apoptotic Cells Measured By TUNEL Assay Analysis (%)
0	DMSO	4.0±0.6	11.0±3.2
	Dex	4.0±0.6	11.0±3.2
1	DMSO	8.2±1.6	10.7±3.2
	Dex	9.9±1.6	12.0±4.5
2	DMSO	7.7±2.3	6.0±1.7
	Dex	10.7±3.5	8.0±1.5
4	DMSO	10.7±0.3	9.3 ±4.1
	Dex	10.2±0.9	11.3 ±3.5
6	DMSO	10.0±0.6	10.3±1.2
	Dex	17.7±0.9 <sup>b</sup>	15.0±1.2
8	DMSO	14.7±1.5	10.0±2.3
	Dex	21.0±2.8 <sup>a</sup>	20.0±2.1 <sup>a</sup>

Values are mean ± SEM of three individual experiments (n=3) representing DMSO and Dex treatment of Nb2 Lymphoma cells at various incubation times

<sup>a</sup>significantly different at  $P \leq 0.05$  vs 0 hour time point, all DMSO controls and 1, 2, 4 and 6 hour Dex treatments

<sup>b</sup>significantly different at  $P \leq 0.05$  vs 0 hour timepoint, 1, 2, 4 and 6 hour DMSO controls and 1, 2 and 4 hour Dex treatments



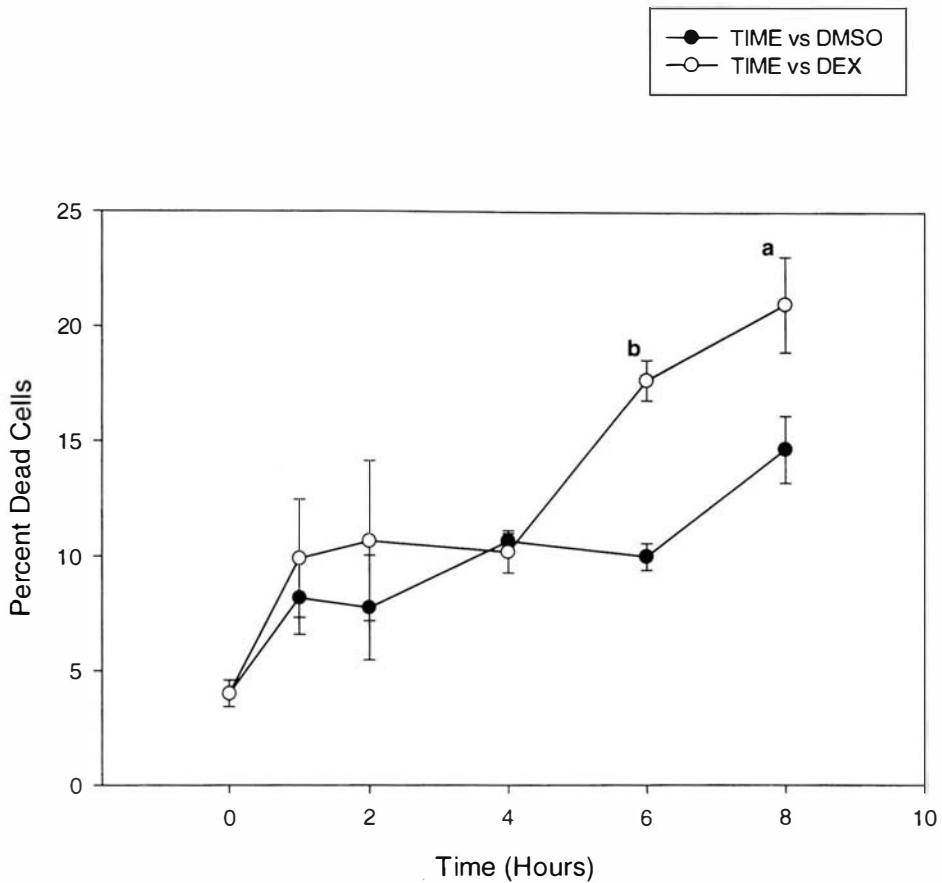


Fig. 5. Trypan Blue Counts of Nb2 Lymphoma cells treated with DMSO and 100nM Dex for various incubation times indicate significant changes ( $P \leq 0.05$  and  $n=3$ ) in the 6 and 8 hour time points as noted by the superscripts (a and b).

<sup>a</sup>significantly different at  $P \leq 0.05$  vs 0 hr timepoint, all DMSO controls and the 1, 2, 4 and 6 hour Dex treatments

<sup>b</sup>significantly different at  $P \leq 0.05$  vs 0 hr timepoint, 1, 2, 4 and 6 hr DMSO controls and 1, 2 and 4 hour Dex treatments

The TUNEL assay indicates that the earliest definitive evidence of Dex-induced apoptosis is visualized at the 8-hour time point (Figure 6). A significant 2-fold increase in the percentage of positively stained cells is seen in the Dex-treated sample over the DMSO sample at 8 hours ( $P \leq 0.05$ ,  $n=3$ ). While not statistically significant, data at 6 hours suggests a 1.5-fold increase in the percentage of positively stained cells in the Dex treated population when compared to the DMSO treated population. Figure 7 displays photomicrographs at 20X objective lens magnification of DMSO and Dex-treated cell populations at the 2 and 8-hour time points. TUNEL labeling is clearly evident at 8 hours (Figure 7D).

Figure 8 exhibits photomicrographs (40X objective magnification) of the TUNEL assay performed on cells treated with DMSO (A), Dex (B), Dex plus Prl (C) and Prl alone (D) after 8 hour incubations. This figure serves as a visual representation of the Dex  $\pm$  Prl effect on Nb2 cells where Dex-induced labeling is inhibited by co-incubation with Prl.

### 3.4 Immunocytochemistry and Antibody Absorption

Immunocytochemical analysis generated from affinity purified polyclonal rabbit antibodies directed against the signal proteins GR, STAT5b, NF $\kappa$ B and I $\kappa$ B $\alpha$  offers evidence for the presence of these respective proteins in the Nb2 cell line. Each antibody of interest stained the cells. Absorption of staining by admixture with 10X free antigen eliminates cell staining.

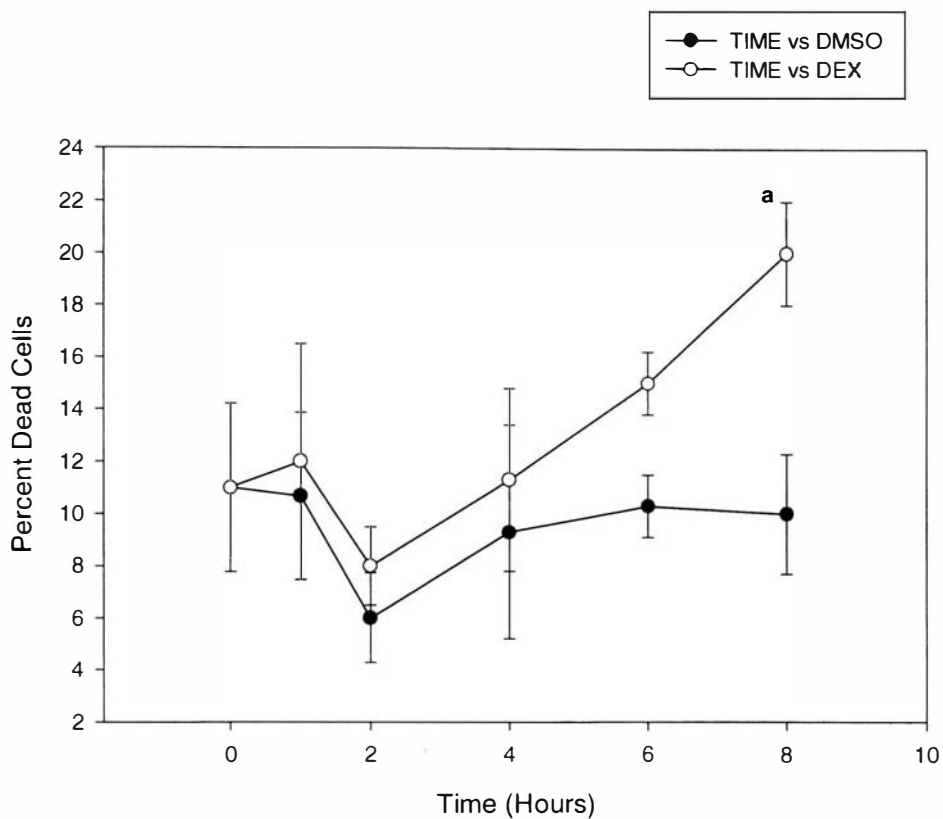
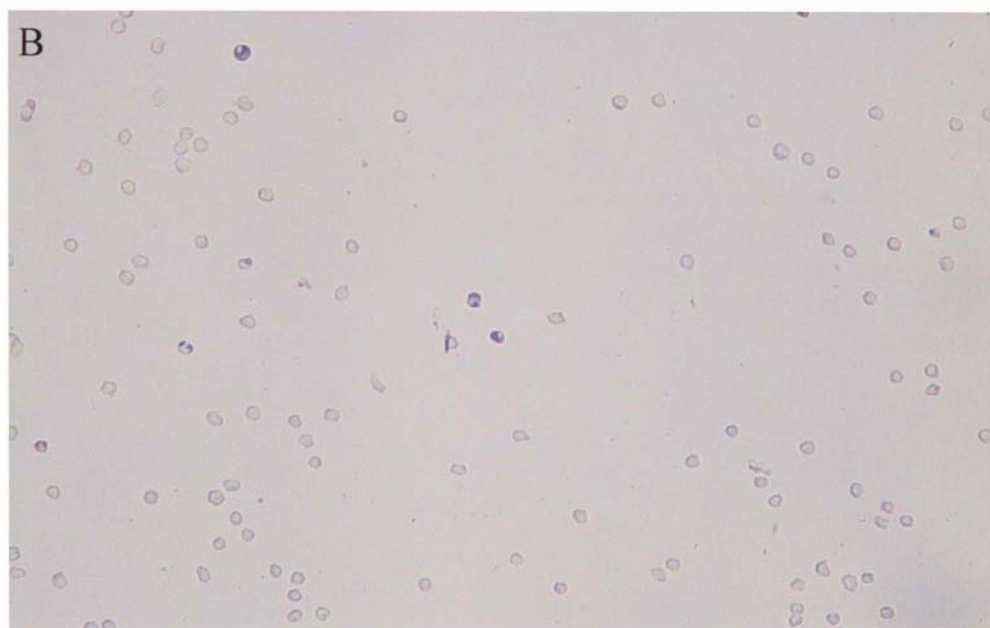
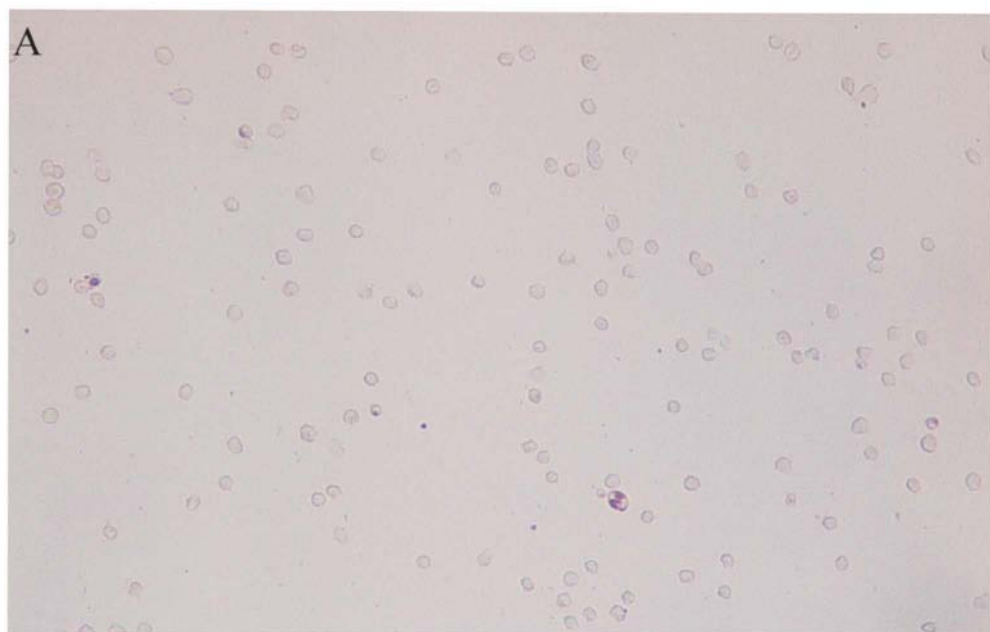


Fig. 6. TUNEL Assay Analysis on Nb2 Lymphoma cells treated with DMSO and 100nM Dex for various incubation time points reveals significant changes ( $P \leq 0.05$  and  $n=3$ ) at the 8 hour time point indicated by the superscript (a).

<sup>a</sup> significantly different at  $P < 0.05$  vs 0 hour time point, all DMSO controls and the 1, 2, 4 and 6 hour Dex treatments

Figure 7. Demonstration of the TUNEL assay performed on the Dex time course assay of Nb2 cells at various time points (177x magnification). A displays the 2-hour DMSO control. B demonstrates TUNEL staining of Dex-treated cells at 2 hours. C displays the 8-hour DMSO control. D shows TUNEL staining of Nb2 cells after 8 hours of Dex treatment. Only at 8 hours, is the difference in the number of stained cells noticeable between DMSO and Dex treatment.



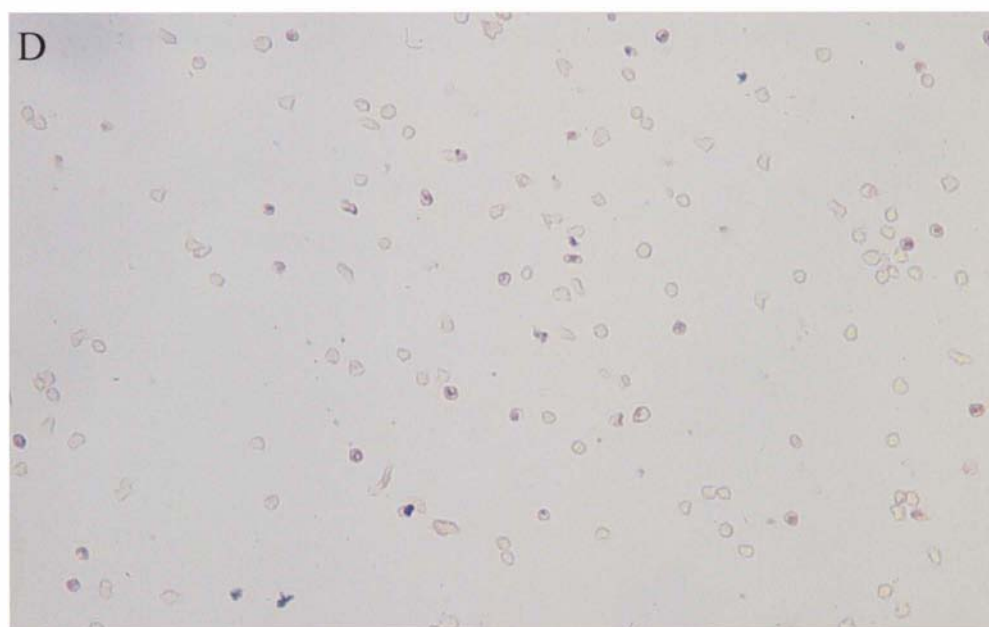
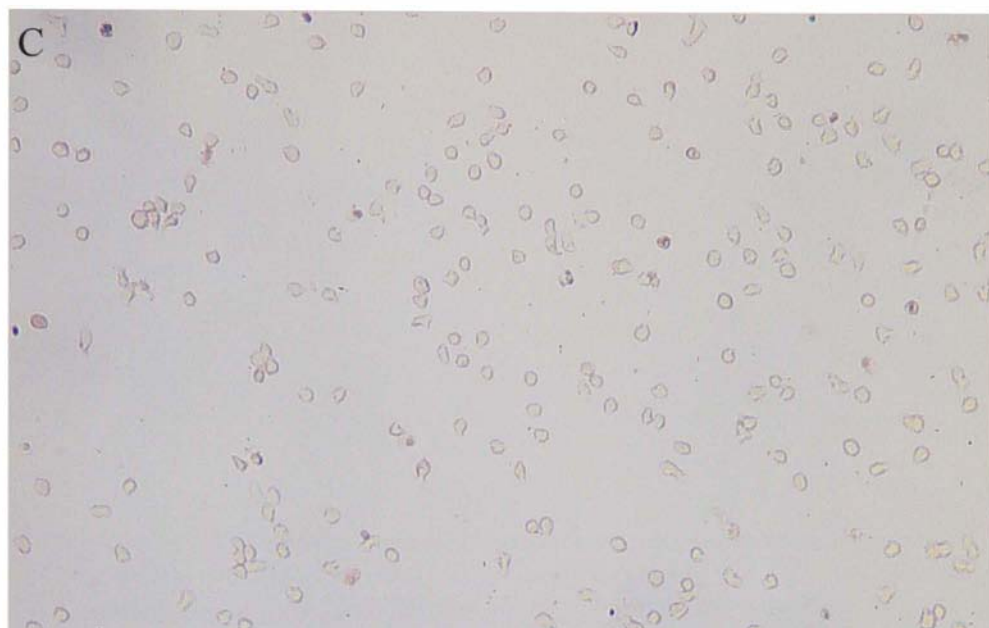
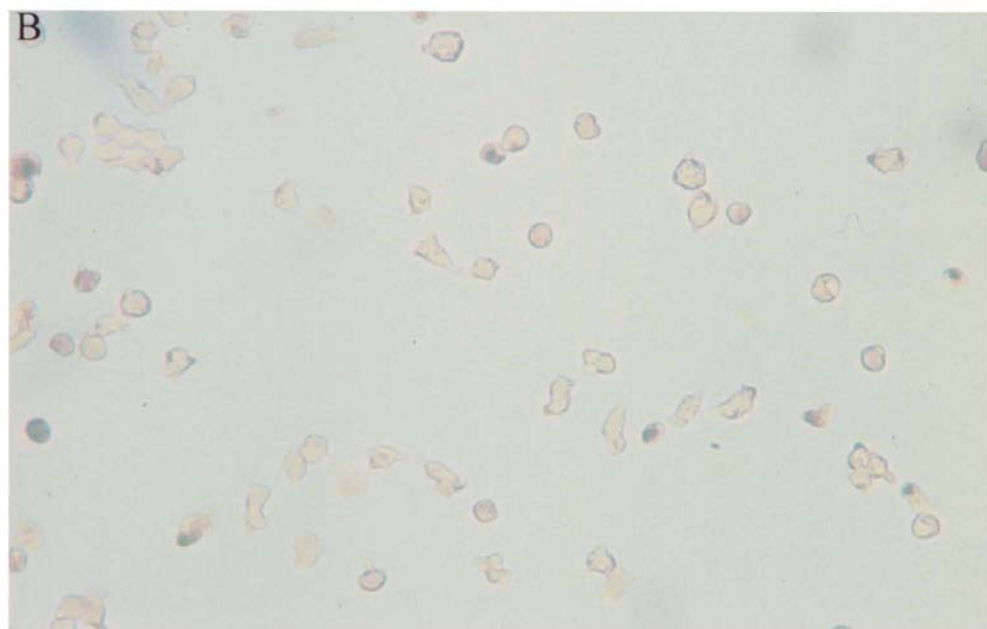
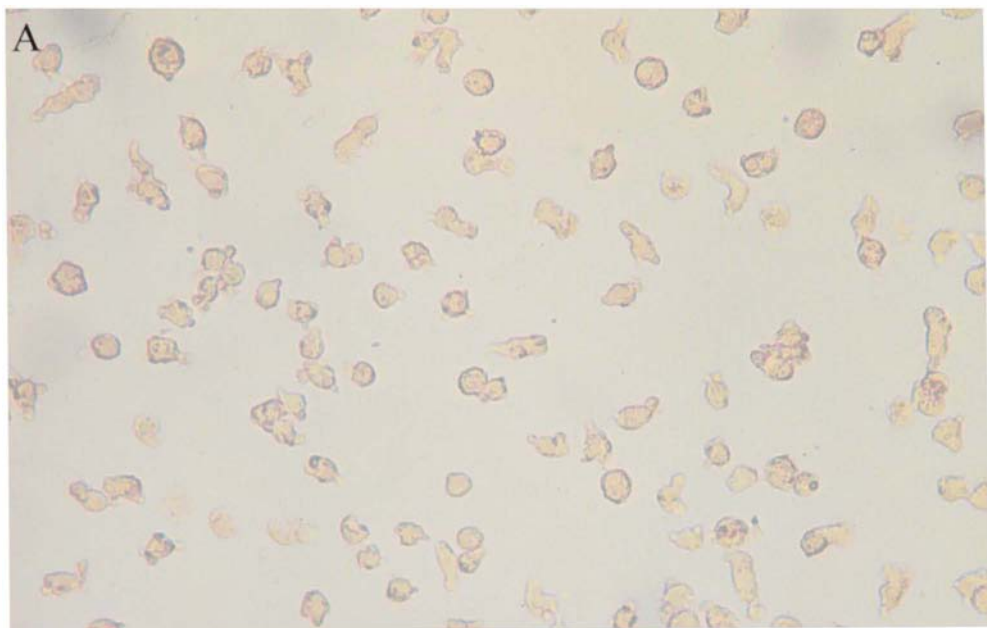
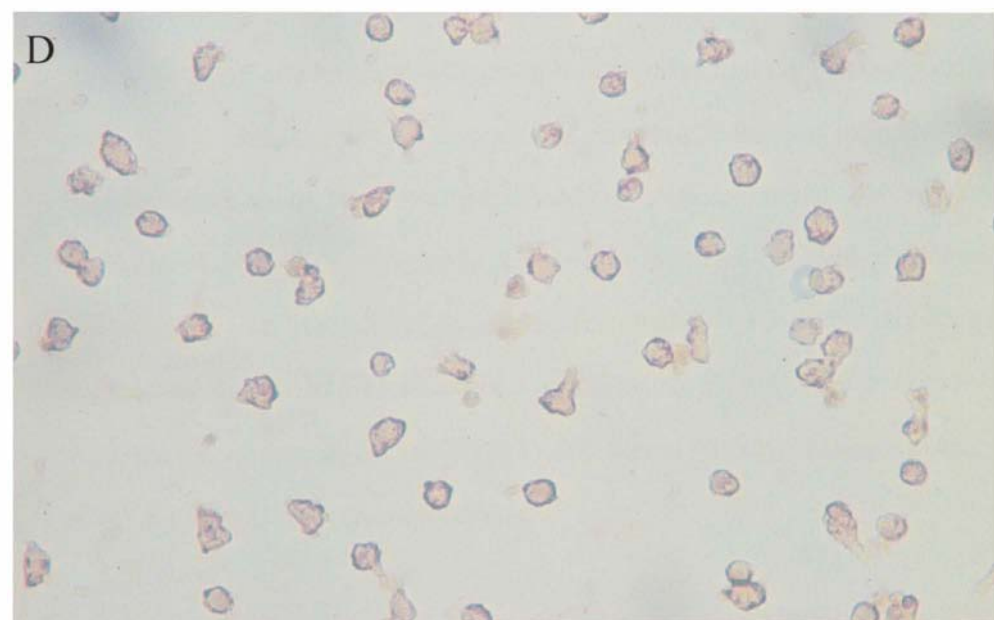
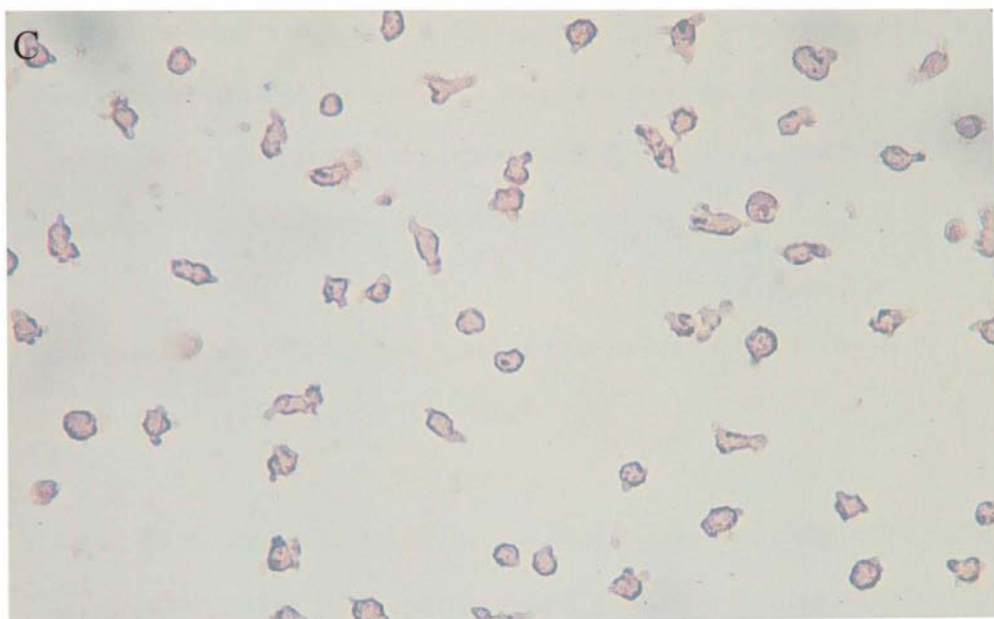


Figure 8. TUNEL staining demonstration (354x magnification) of the effect of DMSO, Dex (100nM), Dex + Prl (1ng/ml) and Prl (1ng/ml) treatment on Nb2 cells at 8 hours. A displays the DMSO control. Except for slight background staining, no apoptotic cells are apparent. B shows an increase in the number of TUNEL stained apoptotic cells as a result of Dex exposure. C exhibits the effect of Dex + Prl co-incubation. Despite background staining, no apoptotic cells are seen. D shows the effect of Prl treatment alone. The background staining in the Dex + Prl and Prl fields appear to be darker than the DMSO fields. Experimental variation and fixation artifact may cause these differences in background staining intensities.







In Figure 9, A and B show anti-GR control and absorbed respectively. Figure 10, A and B display anti-STAT5b control and absorbed respectively. Figure 11, A and B exhibit anti-NFkB control and absorbed respectively. Figure 12, A and B demonstrate anti-IkB $\alpha$  control and absorbed respectively.

### 3.5 Examination of the Immunocytological Changes in Antibody Staining in Response to the Dex Time Course Assay

Tables 2-5 show the quantified results of antibody staining directed against the signal proteins GR, STAT5b, NFkB and IkB $\alpha$  following DMSO or Dex treatments for 0, 1, 2, 4, 6 and 8 hours (table 2; anti-GR, table 3; anti-STAT5b, table 4; anti-NFkB and table 5; anti-IkB $\alpha$ ). In response to the different treatments and the various lengths in incubation times, data reflect the changes in both the percentages of positively stained cells and the percentages of centrally localized stained cells with each antibody.

Based upon our results, the percentages of total cells stained were approximately 40% for each antibody. Of the cells that were stained for each antibody, most of the stain was localized to the periphery of the cell. Statistical analysis reveals that centralized staining with anti-GR at the 8-hour time point showed the only significant change above the 0-hour controls and the 2-hour DMSO control ( $P \leq 0.05$ ). Changes in the other antibodies tested were not significant.

Figure 9. A demonstrates staining of Nb2 cells with antibody directed against GR at a concentration of 2ug/ml. B shows the disappearance of staining when absorbed out with specific antigen at a peptide concentration of 20ug/ml. Magnification x354.

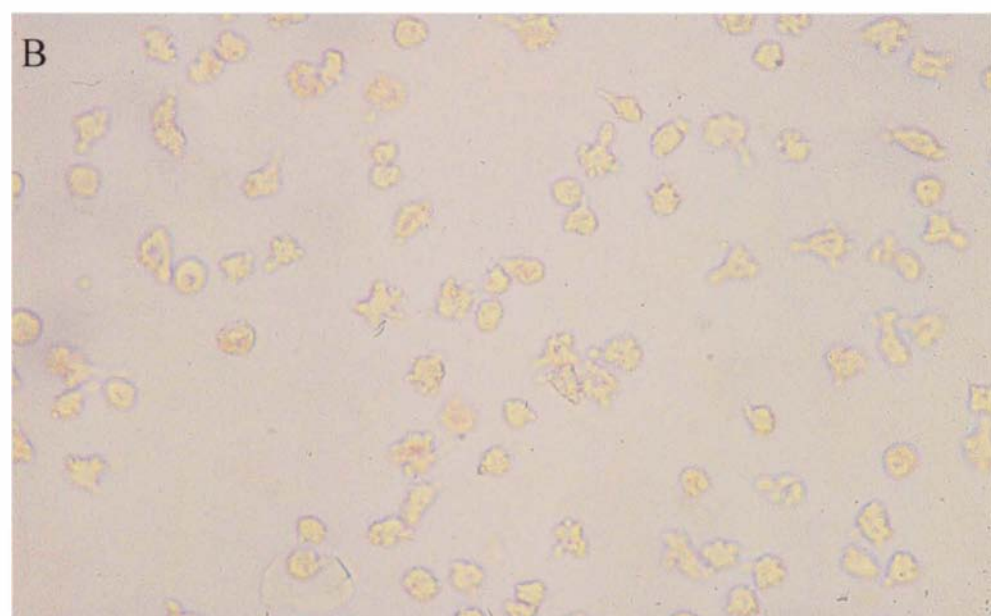
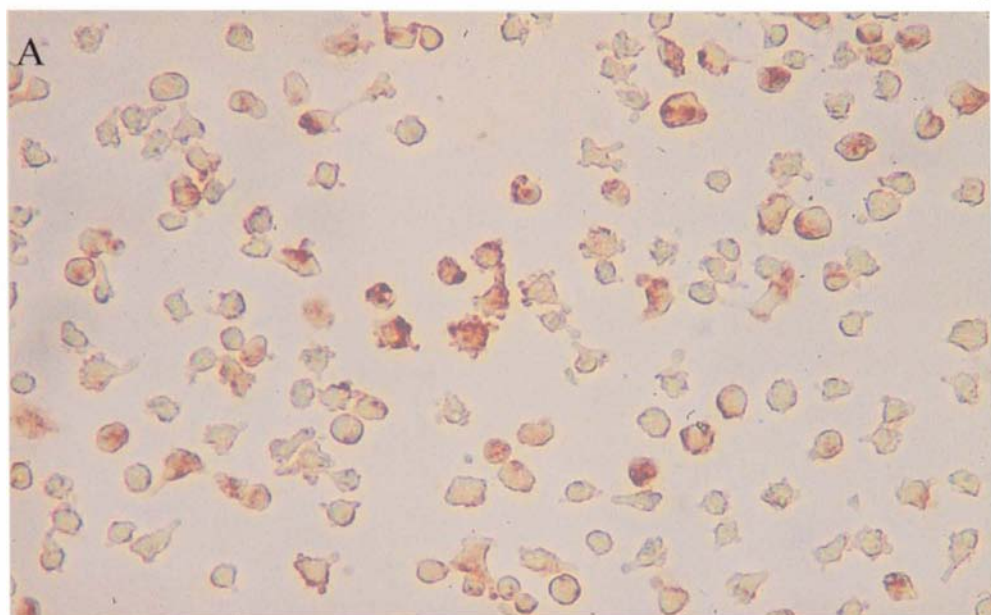


Figure 10. A demonstrates staining of Nb2 cells with antibody directed against STAT5b at a concentration of 2ug/ml. B shows the disappearance of staining when absorbed out with specific antigen at a peptide concentration of 20ug/ml. Magnification x354.

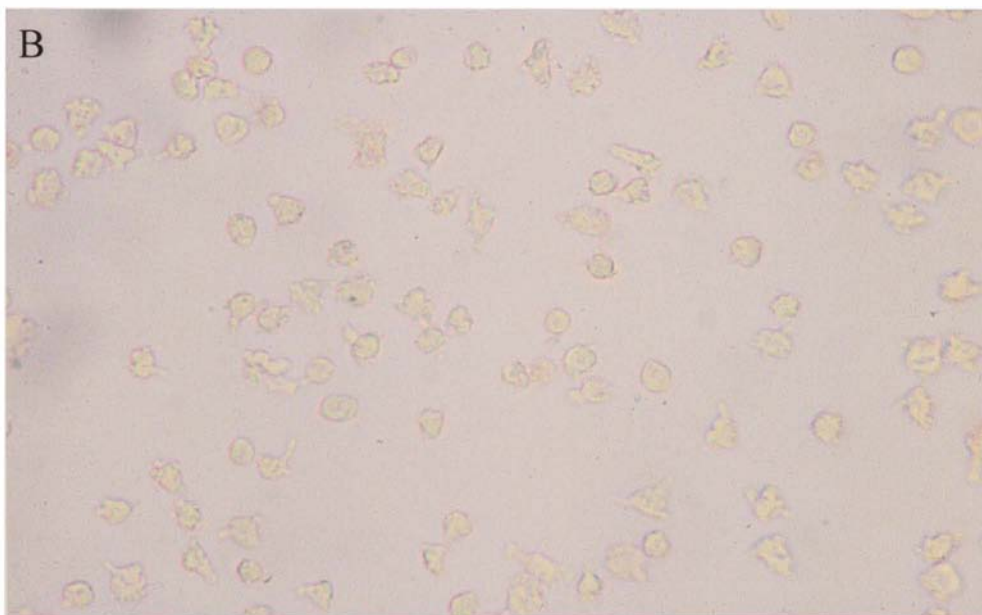
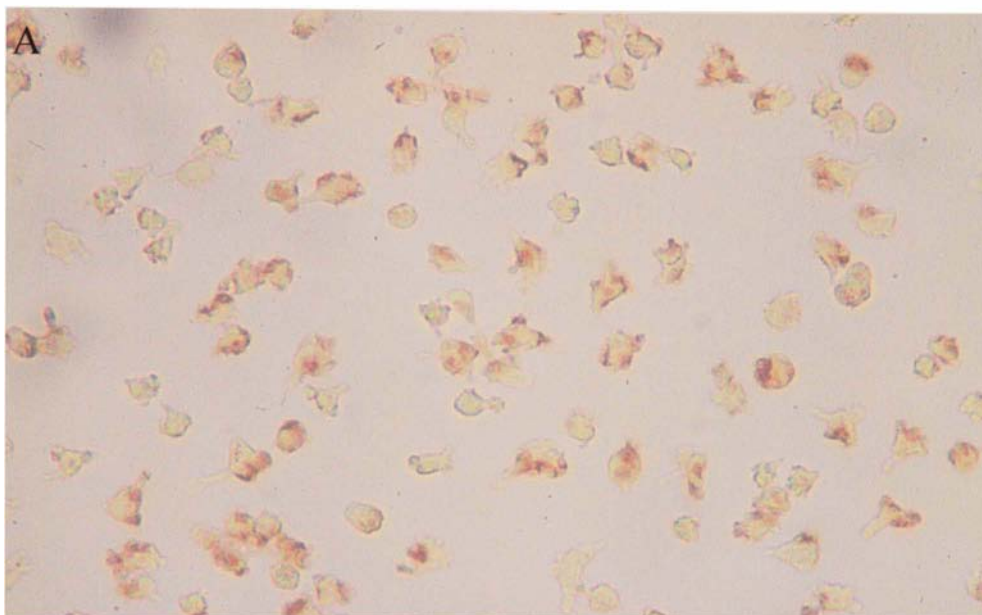


Figure 11. A demonstrates staining of Nb2 cells with antibody directed against NFkB at a concentration of 2ug/ml. B shows the disappearance of staining when absorbed out with specific antigen at a peptide concentration of 20ug/ml. Magnification x354.

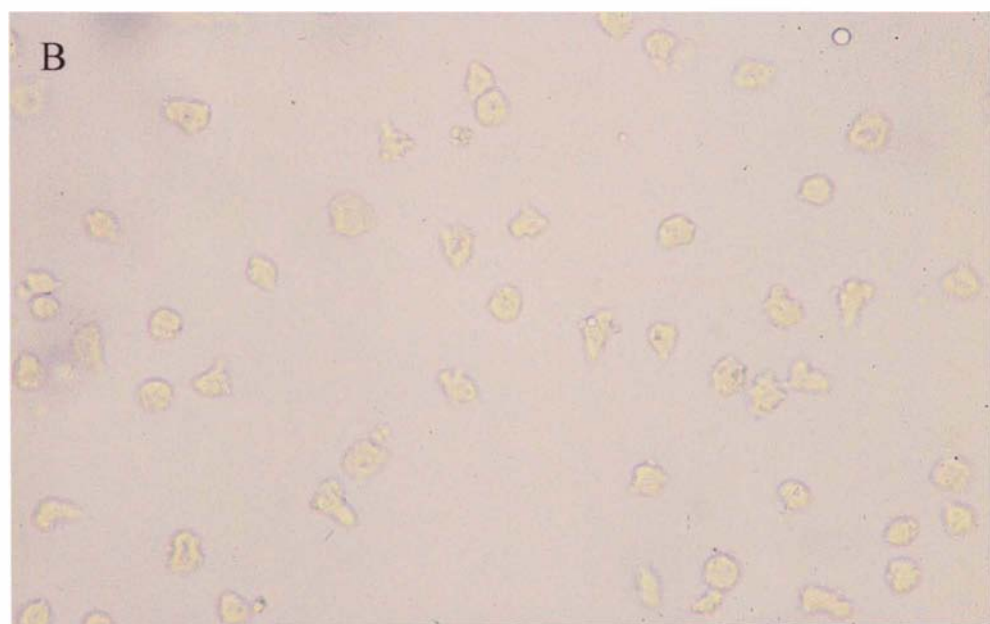
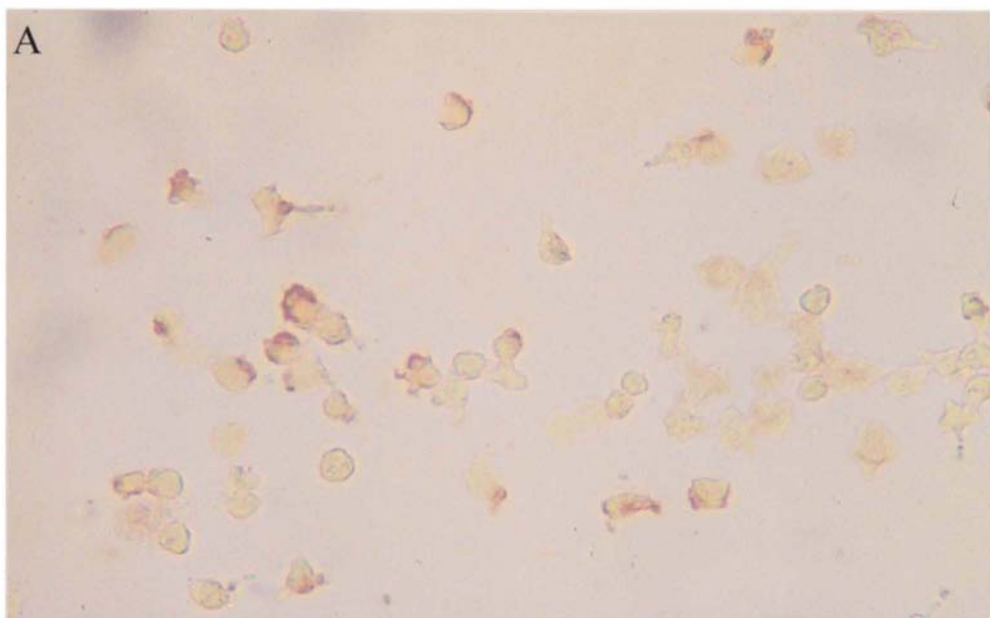




Figure 12. A demonstrates staining of Nb2 cells with antibody directed against I $\kappa$ B $\alpha$  at a concentration of 2 $\mu$ g/ml. B shows the disappearance of staining when absorbed out with specific antigen at a peptide concentration of 20 $\mu$ g/ml. Magnification x354.

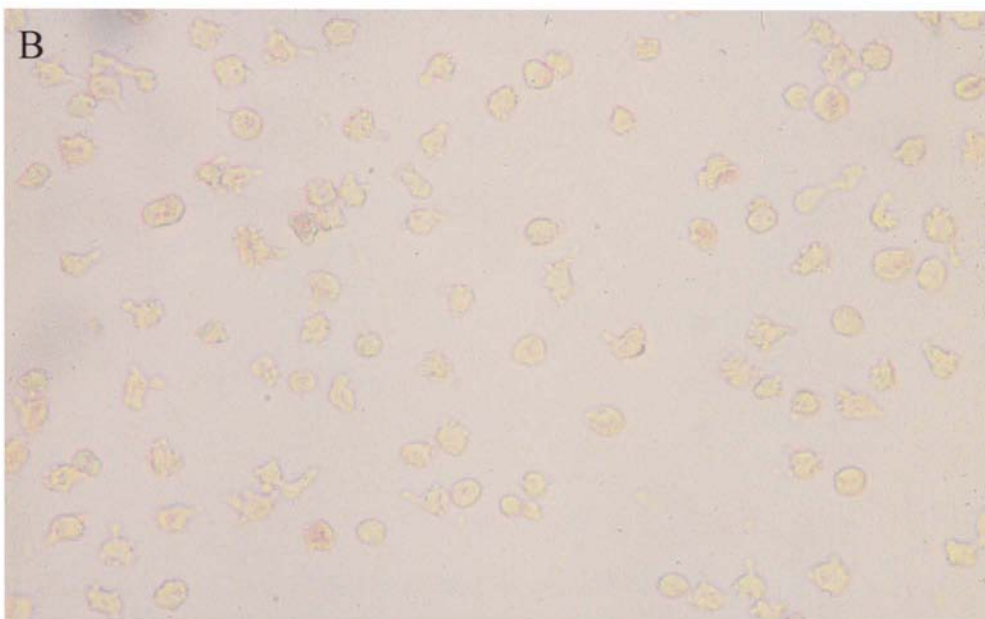
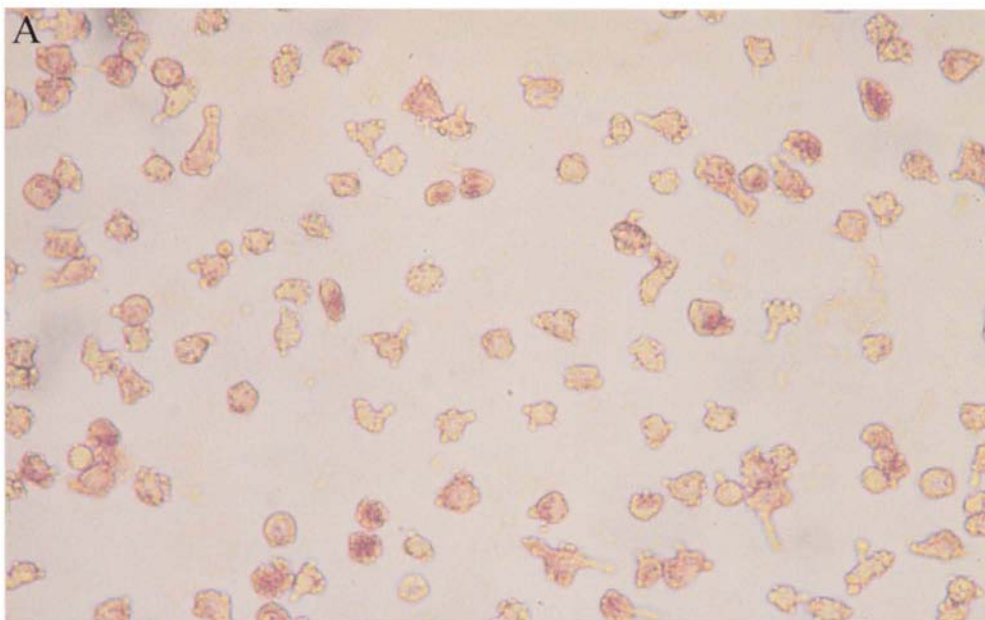


Table 2. Immunocytochemical Quantification of Nb2 Lymphoma Cells Stained for Anti-GR after DMSO and Dex Treatment for Various Incubation Periods

Time (Hours)	Treatment	Percent Cells Stained for Anti-GR (%)	Percent Cells with Centrally Localized Stain (%)
0	DMSO	41.7 $\pm$ 1.5	2.6 $\pm$ 0.3
	Dex	41.7 $\pm$ 1.5	5.0 $\pm$ 1.0
1	DMSO	40.7 $\pm$ 1.5	5.2 $\pm$ 1.2
	Dex	40.7 $\pm$ 0.9	7.3 $\pm$ 1.5
2	DMSO	40.3 $\pm$ 1.3	3.0 $\pm$ 0.6
	Dex	45.0 $\pm$ 1.2	4.0 $\pm$ 0.6
4	DMSO	43.3 $\pm$ 0.9	4.3 $\pm$ 1.3
	Dex	44.0 $\pm$ 0.6	6.3 $\pm$ 1.9
6	DMSO	42.7 $\pm$ 3.3	4.7 $\pm$ 0.3
	Dex	44.3 $\pm$ 3.0	5.3 $\pm$ 0.3
8	DMSO	27.3 $\pm$ 3.7	4.7 $\pm$ 0.7
	Dex	42.0 $\pm$ 0.3	8.3 $\pm$ 2.0 <sup>a</sup>

Values are mean  $\pm$  SEM of three individual experiments (n=3)

<sup>a</sup>significantly different at  $P \leq 0.05$  vs 0 hour control and the 2 hour DMSO control

Table 3. Immunocytochemical Quantification of Nb2 Lymphoma Cells Stained for Anti-STAT5b after DMSO and Dex Treatment for Various Incubation Periods

Time (Hours)	Treatment	Percent Cells Stained for Anti-STAT5b (%)	Percent Cells with Centrally Localized Stain (%)
0	DMSO	44.0 $\pm$ 1.5	3.0 $\pm$ 0.6
	Dex	41.0 $\pm$ 1.5	2.7 $\pm$ 1.2
1	DMSO	41.3 $\pm$ 1.2	3.3 $\pm$ 0.7
	Dex	42.3 $\pm$ 3.2	5.3 $\pm$ 2.0
2	DMSO	38.0 $\pm$ 5.0	2.7 $\pm$ 1.2
	Dex	36.0 $\pm$ 4.0	2.7 $\pm$ 1.2
4	DMSO	41.3 $\pm$ 0.3	4.0 $\pm$ 1.0
	Dex	37.3 $\pm$ 3.7	4.0 $\pm$ 1.5
6	DMSO	39.3 $\pm$ 2.3	3.7 $\pm$ 1.5
	Dex	41.7 $\pm$ 3.3	3.6 $\pm$ 0.3
8	DMSO	39.0 $\pm$ 4.4	4.0 $\pm$ 0.6
	Dex	38.0 $\pm$ 3.2	5.3 $\pm$ 0.9

Values are mean  $\pm$  SEM of three individual experiments (n=3).

Table 4. Immunocytochemical Quantification of Nb2 Lymphoma Cells Stained for Anti-NFkB after DMSO and Dex Treatment for Various Incubation Periods

Time (Hours)	Treatment	Percent Cells Stained for Anti-NFkB (%)	Percent Cells with Centrally Localized Stain (%)
0	DMSO	43.3 $\pm$ 1.0	7.0 $\pm$ 3.1
	Dex	39.0 $\pm$ 1.7	4.3 $\pm$ 1.9
1	DMSO	43.7 $\pm$ 1.2	5.7 $\pm$ 4.2
	Dex	43.2 $\pm$ 2.1	9.3 $\pm$ 5.0
2	DMSO	42.0 $\pm$ 2.9	3.3 $\pm$ 1.3
	Dex	42.3 $\pm$ 2.3	3.0 $\pm$ 0.6
4	DMSO	40.3 $\pm$ 1.2	4.3 $\pm$ 1.2
	Dex	43.3 $\pm$ 1.7	7.0 $\pm$ 1.5
6	DMSO	42.7 $\pm$ 0.3	3.3 $\pm$ 0.3
	Dex	44.7 $\pm$ 1.3	4.0 $\pm$ 1.5
8	DMSO	42.7 $\pm$ 0.3	7.6 $\pm$ 2.4
	Dex	42.7 $\pm$ 0.9	6.7 $\pm$ 2.3

Values are mean  $\pm$  SEM of three individual experiments (n=3).

Table 5. Immunocytochemical Quantification of Nb2 Lymphoma Cells Stained for Anti-IkB $\alpha$  after DMSO and Dex Treatment for Various Incubation Periods

Time (Hours)	Treatment	Percent Cells Stained for Anti- IkB $\alpha$ (%)	Percent Cells with Centrally Localized Stain (%)
0	DMSO	39.0 $\pm$ 0.0	3.7 $\pm$ 0.3
	Dex	40.0 $\pm$ 2.1	6.0 $\pm$ 1.5
1	DMSO	43.0 $\pm$ 1.2	10.0 $\pm$ 4.5
	Dex	43.3 $\pm$ 1.3	9.3 $\pm$ 3.9
2	DMSO	43.0 $\pm$ 2.1	4.3 $\pm$ 1.9
	Dex	39.7 $\pm$ 3.2	4.3 $\pm$ 1.5
4	DMSO	42.0 $\pm$ 0.6	4.0 $\pm$ 1.5
	Dex	43.0 $\pm$ 1.0	5.6 $\pm$ 1.5
6	DMSO	44.0 $\pm$ 1.5	5.7 $\pm$ 1.7
	Dex	41.0 $\pm$ 0.3	5.3 $\pm$ 0.3
8	DMSO	41.0 $\pm$ 0.6	9.0 $\pm$ 3.5
	Dex	41.0 $\pm$ 1.5	9.7 $\pm$ 3.7

Values are mean  $\pm$  SEM of three individual experiments (n=3).

## Chapter 4

### DISCUSSION

As was introduced earlier, the main objective of this study was to test the feasibility of the morphological approach in the investigation of apoptosis control. The model used for this approach was the Nb2 lymphoma cell. In this cell line, an antagonistic interaction exists between glucocorticoids and Prl; individually, glucocorticoid treatment induces apoptosis while Prl treatment induces mitogenesis. When applied together, glucocorticoids block Prl-induced mitogenesis while, concomitantly, Prl inhibits Dex-induced apoptosis (Fletcher-Chiappini et al., 1993). This interaction makes this cell line a dynamic model from which to examine programmed cell death. With the morphological approach, we were able to achieve several objectives. First, we determined whether the TUNEL assay could be used for the qualitative and quantitative assessment of apoptosis in the Nb2 cell. Second, we examined the apoptosis-associated signal proteins GR (the signal for Dex), STAT5b (the signal for Prl), NFkB and Ikb $\alpha$  (two signals associated in glucocorticoid-induced apoptosis) in the Nb2 cell through the use of immunocytochemistry (ICC). With this method, we were able to both demonstrate specific antibody staining of the protein signals of

interest and to determine whether changes in these signals could be visualized under conditions affecting apoptosis.

One problem initially encountered using the morphological approach involved developing a method of cell quantification best suited for the TUNEL assay and ICC. Based upon earlier literature surveys, the majority of the methodologies used for quantification revolved around biochemical and molecular biological protocols. These protocols involved cell homogenization and were not well tailored for the morphological approach. A novel methodology was needed that would benefit the morphological approach; one that would provide a reliable and consistent assessment of the morphological changes visualized with the TUNEL assay and ICC. As a result, we developed a method of quantification that was loosely based on hemacytometer cell counting (ie. The distribution of morphological characteristics in a flat field of cells). Approximately 60,000 fixed cells were spotted in a 10ul volume onto each 5mm etched circle on the slides to obtain representative cell samplings. After the TUNEL Assay or immunostaining, photomicrographs at 20X or 40X objective magnification were taken of four cell fields (close to the center of the circle) situated at positions corresponding to 2, 4, 8 and 10 o'clock in each etched circle. The same template pattern was followed for each different cell treatment. The cells were then manually counted from the photomicrographs for total cell number, number of positively stained cells and the number of cells exhibiting centralized staining. The total number of cells counted from each sample ranged from 400 to 1,600 cells. Our



objective was to obtain a reasonably accurate quantification of the features of interest (eg. percentage apoptosis or percentage immunostaining in the cell sample).

According to our results, our method of quantification of cell proportionality appears to be valid. As can be seen in Tables 1-5, relatively small standard errors in the values are recorded for each cell treatment for both the TUNEL assay and ICC suggesting consistent results from one experiment to the next. Furthermore, the method appears to be able to detect relatively modest statistically significant increases in Dex-induced apoptosis (8-hour time point). ICC data also suggests a statistical difference in GR centralized staining that may reflect nuclear translocation at 8 hours.

Based upon the results from the 24-hour Dex  $\pm$  Prl assay (Figure 2), Trypan Blue exclusion counts confirm earlier results from studies performed by Fletcher-Chiappini in which 100nM Dex treatment dramatically increases cell cytolysis above baseline DMSO levels; about a 2.75-fold increase in cell death (Fletcher-Chiappini et al., 1993). Co-incubation with Prl inhibits this effect. These results verify that the Nb2 cells, in regard to Dex/ Prl-responsiveness, have retained their typical characteristics as was seen in previous studies performed in our laboratory (Fletcher-Chiappini et al., 1993). This verification in cell behavior was necessary to determine whether the Nb2 cell batch that was received from outside laboratory sources exhibited unchanged or altered characteristics with regard to hormonal control of cytolysis.

The photomicrographs of the TUNEL assay performed on the 24-hour Dex experiment (Figures 3 and 4) demonstrates the utility of the TUNEL assay in detecting apoptosis in log phase, non-synchronized cells. A definitive increase in the number of stained cells in the Dex sample can be seen over the DMSO control. Furthermore, the TUNEL staining in Figure 4 highlights the morphology of cells undergoing apoptosis. Some of the apoptotic cells exhibit dark staining of fragmented chromatin encapsulated in the large nucleus. As is apparent, this large nucleus comprises the majority of the volume of the lymphoma cell. Other apoptotic cells seen in the field are at later stages of death and exhibit apoptotic vesicles or bodies. Apoptotic vesicles are remnants of the fragmented nucleus (Wyllie et al., 1980).

The purpose of the Dex exposure in synchronized Nb2 cells is to determine whether the TUNEL assay could detect apoptosis and its onset time. Based upon our results from Table 1 and Figures 5 and 6, a strong correlation between the TUNEL assay and Trypan Blue exclusion may be seen. Both methods indicate significant increases in the percentages of dead cells at 8 hours and possibly at 6 hours. This correlation is unexpected because of the presumed differences in the mechanisms reflected by these two methods; one would expect to detect apoptosis with the TUNEL assay earlier than with Trypan Blue exclusion (the latter being the least specific for detecting apoptosis). As was previously established, these two methods were implemented to detect and measure the percentages of cells undergoing Dex-induced cytolysis, most

likely caused by apoptosis. According to Perry et al. (1997), the TUNEL assay detects apoptosis by labeling DNA fragmentation while Trypan Blue detects cell death by detecting loss of selective plasma membrane permeability. Presumably, DNA fragmentation is an early event in apoptosis that proceeds the loss of selective plasma membrane permeability (Kerr et al., 1991, Majino et al., 1995, Perry et al., 1997). In fact, the membranes of these apoptotic cells do not lyse until late in the apoptotic pathway (Kerr et al., 1991, Majino et al., 1995, Perry et al., 1997).

Furthermore, studies performed independently by Fletcher and LaVoie show that apoptosis is first detectable in synchronized Nb2 cells by agarose gel electrophoresis or diphenylamine DNA fragmentation assay after 4 hours of Dex incubation (Fletcher Ph. D. thesis, LaVoie, Ph. D. thesis). Both Trypan Blue exclusion counts and the TUNEL assay in our study show that the onset of apoptosis appears to occur after 6 or 8 hours of Dex incubation. The discrepancy between the onset time of apoptosis recorded by DNA fragmentation and our morphological techniques may have several explanations. First of all, ICC and functional data suggests that Nb2 cells are heterogeneous with regard to GR and glucocorticoid responsiveness. We see that about 40% of the synchronized Nb2 cells are positive for GR. These data imply that the cell population is diluted with GR negative cells. Consistently, the same approximate proportion of cells dies after 24 hours of Dex treatment. Thus, only a fraction of the cell population responding to Dex treatment is undergoing apoptosis. As a result, at earlier incubation time points, significant increases in the percentages

of cell death may not have appeared between Dex and DMSO treatments or may have been difficult to detect. Hence, we observe a later onset time of apoptosis.

Second, as a result of multiple cell passings, the Nb2 subculture may have become less responsive to Dex treatment. Although the magnitude of Dex induced cytolysis observed in this study is consistent with previous work (Fletcher-Chiappini et al., 1993, Witorsch et al., 1993), there may be as yet undetected kinetic differences in Dex responsiveness between the cells currently in use and those used previously. Finally, the TUNEL assay, in our hands, may not be as sensitive as DNA fragmentation/agarose gel electrophoresis in detecting apoptosis. The comparative sensitivities of DNA fragmentation relative to the TUNEL assay in our study contradict the findings of Gavrieli, who reports that the TUNEL assay is the more sensitive of the two assays (Gavrieli et al., 1992). No explanations for differences seen between our observations and those of Gavrieli can be offered except for the differences in the cell types being studied. Gavrieli harvested thymocytes from male Sabra rats in his studies (Gavrieli et al., 1992) while we studied Nb2 lymphoma cells from male Nobel rats. Neoplastic cells may be inherently more resistant to apoptotic-inducing stimuli (such as Dex) than normal cells.

With ICC, we were able to demonstrate staining of signal proteins of interest (GR, STAT5b, NFkB and I $\kappa$ B $\alpha$ ) in the Nb2 cell with polyclonal antibodies. These antibodies were affinity purified by the supplier to minimize nonspecificity and react

with highly specific peptide sequences (about 20 amino acids in length) on their respective proteins. In order to confirm specificity of these antibodies in Nb2 cells, antibodies were premixed and incubated with their respective antigens (eg. Peptide sequences). Application of the antibody/peptide mixture to Nb2 cells in an ICC assay resulted in the inhibition of cell staining. Antibody absorption is a stringent method of establishing specificity of antibody binding in cells (Witorsch, 1980). In order to further verify specificity, several of these antibodies were cross-absorbed with different antigens and failed to diminish immunostaining (unpublished observations).

As discussed earlier, our morphological approach was implemented to determine the proportion of stained cells, the localization of signals within the cell (central vs. peripheral), and whether any changes could be detected at time points proceeding the onset of Dex-induced apoptosis. In theory, changes in these particular signal proteins, if they occur, should proceed apoptosis onset. However, we observed approximately the same percentage of cells (40%) stained with antibodies directed against GR, STAT5b, NFkB and Ikb $\alpha$  in log phase and in synchronized cells for all of the time points with and without Dex exposure.

The percentage of cells stained positive for GR (41%) seems consistent with the percentage of Dex-induced cell death observed herein and reported previously (Fletcher-Chiappini et al., 1993, Witorsch et al., 1993). A similar proportion of Ikb $\alpha$  stained cells is concordant with notion that GR induces transcription of Ikb $\alpha$

(Scheinman et al, 1995). In addition, the similar proportion of cells staining positive for NF $\kappa$ B is consistent with the functional linkage (or antagonistic relationship) between this signal and I $\kappa$ B $\alpha$  (Israel, 1995). Multiple immunostaining of these signals to co-localize them to the same cell would help to verify the functional relationship between GR, I $\kappa$ B $\alpha$  and NF $\kappa$ B.

The percentage of STAT5B (the signal associated with Prl action) positive log phase Nb2 cells is lower than would be expected in view of the Nb2 cell dependence on and sensitivity to lactogenic hormones (Gout et al., 1986). This low percentage of STAT5b staining might suggest that alternate signals (STAT5a, STAT1, STAT3 and MAP Kinase) may exist which also mediate these Prl-induced effects (Yu-Lee, 1997). On the other hand, STAT5b immunostaining might suggest that only a subset of Nb2 cells are Prl responsive and then, in turn, release diffusable extracellular signals to surrounding Prl unresponsive cells to effect cellular responses.

In addition to the lack of change in the proportion of cells stained, few if any changes were observed in the intracellular distribution (i.e. peripheral to central) of staining or staining intensity for the signals of interest due to synchronization and/or Dex treatment. One would have expected, with Dex treatment, perhaps, an intensification of I $\kappa$ B $\alpha$  staining (Scheinman et al., 1995) and or a redistribution of GR staining from periphery to the center of the cell (reflecting nuclear translocation) prior to the onset of Dex-induced apoptosis. Previous studies, both biochemical and morphological

attempted to show nuclear translocation via electrophoretic mobility-shift assays (Tanaka et al., 1992), radiolabeling of homogenized cells (Kaufmann, et al., 1982), immunoprecipitation assays (Tanaka et al., 1996), direct fluorescence microscopy with glucocorticoid receptor-green fluorescent protein fusion (GR-GFP) (Carey et al., 1996), light microscopy, electron microscopy and RNA hybridization to DNA response elements (Antakly et al., 1989). However, these studies failed to provide adequate quantification of their observations. Based upon our observations, the only statistically significant change appears to be an increase in centralized GR staining after 8 hours of Dex treatment compared to the 0-hour control. It is uncertain whether this reflects true nuclear translocation of GR or condensation of nuclear material in apoptotic cells.

Since the immunostaining observed herein was specific for the signals in question, the failure to detect changes in the proportion of cells immunostained suggests that this proportionality in log phase cells is unaffected by synchronization and Dex treatment. The failure to demonstrate changes in intensity and intracellular distribution probably reflects the need to refine or modify this methodology. It is noteworthy that the preparations currently under examination are whole cells viewed from a three-dimensional perspective in which it is difficult to differentiate nucleus from overlying membrane and cytoplasm.

In conclusion, the morphological approach proves to be a valuable tool from which to study apoptosis. However, it does have its limitations at this time. Visualization of signal redistribution may require techniques such as confocal microscopy and/or immunocytochemistry of sectioned paraffin embedded cells. In doing so, the changes in these intracellular signals preceding and accompanying apoptosis may be detected. Furthermore, to provide a more precise and accurate Dex response in the Nb2 cells, procedures are underway (i.e. limiting dilution) to develop a homogeneous subline of enriched GR positive Nb2 cells. With these improvements, the morphological approach implemented in concert with biochemical approaches may provide further insight into the signaling cascade involved in the induction of apoptosis.



## **LIST OF REFERENCES**

## LIST OF REFERENCES

Antakly, T., Thompson, E.B. and O'Donnell, D. Demonstration of the Intracellular Localization and Up-Regulation of Glucocorticoid Receptor by *in Situ* Hybridization and Immunocytochemistry. *Cancer Research*. Sup 49:2230s, 1989.

Arends, M.J., Morris, R.G. and Wylie, A.H. Apoptosis: The Role of the Endonuclease. *Am. J. of Path.* 136(3):593, 1990.

Auphan, N., DiDonato, J.A., Rosette, C., Helmsberg, A. and Karin, M. Immunosuppression by Glucocorticoids: Inhibition of NF $\kappa$ B Activity Through Induction of I $\kappa$ B Synthesis. *Science*. 270:286, 1995.

Barinaga, M. Life-Death Balance Within the Cell. *Science*. 274:724, 1996.

Beg, A.A. and Baltimore, D. An Essential Role for NF $\kappa$ B in Preventing TNF- $\alpha$ -Induced Cell Death. *Science*. 274:782, 1996.

Brown, K., Gerstberger, S., Carlson, L., Granzoso, G. and Siebenlist, U. Control of I $\kappa$ B $\alpha$  Proteolysis by Site-Specific, Signal-Induced Phosphorylation. *Science*. 267:1485, 1995.

Brusch, W., Kleine, L. and Tenniswood, M. The Biochemistry of the Cell Death by Apoptosis. *Biochem. Cell. Biol.* 88:1071, 1990.

Camarillo, I.G., Linebaugh, B.E. and Rillema, J.A. Differential Tyrosyl-Phosphorylation of Multiple Mitogen-Activated Protein Kinase Isoforms in Response to Prolactin in Nb2 Lymphoma Cells. *P.S.E.B.M.* 215:198, 1997.

Carey, K.L., Richards, S.A., Lounsbury, K.M. and Macara, I.G. Evidence Using a Green Fluorescent Protein-Glucocorticoid Receptor Chimera That the Ran/TC4 GTPase Mediates an Essential Function Independent of Nuclear Protein Import. *J. Cell Biol.* 133(5):985, 1996.

Compton, M. and Cidlowski, J. Rapid *in Vivo* Effects of Glucocorticoids on the Integrity of Rat Lymphocyte Genomic Deoxyribonucleic Acid. *Endocrinology*. 118:38, 1986.

- Duncan, D.B. Multiple Range and Multiple F tests. *Biometrics*. 11:1, 1955.
- Duvall, E. and Wyllie, A.H. Death and the Cell. *Immunol Today*. 7:115, 1986.
- Fleming, H.F., Pettigrew, N.M., Matusik, J.R. and Friesen, H.G. Thymic Origin of the Prolactin-Dependent Nb2 Lymphoma Cell Line. *Cancer Research*. 42:3138, 1982.s
- Fletcher, S.E. Prolactin-Glucocorticoid Interactions in Nb2 Lymphoma Cells. Ph.D. thesis. Virginia Commonwealth University, 1991.
- Fletcher-Chiappini, S.E., Compton, M.M., LaVoie, H.A., Day, B.E. and Witorsch, R.J. Glucocorticoid-Prolactin Interactions in Nb2 Lymphoma Cells: Antiproliferative versus Anticytolytic Effects. *P.S.E.B.M.* 202:245, 1993.
- Flomerfelt, F.A. and Miesfeld, R.L. Recessive Mutations in a Common Pathway Block Thymocyte Apoptosis Induced by Multiple Signals. *The J. of Cell Biol.* 127(6):1729, 1994.
- Gavrieli, Y., Sherman, Y. and Ben-Sasson, S.A. Identification of Programmed Cell Death In Situ via Specific Labeling of Nuclear DNA Fragmentation. *The J. of Cell Biol.* 119(3):493, 1992.
- Gerschenson, L.E. and Rotello, R.J. Apoptosis: A Different Type of Cell Death. *F.A.S.E.B. J.* 6:2450, 1992.
- Gold, R., Schmied, M., Giegerich, G., Breitschopf, H., Gartung, H.P., Toyka, V.K. and Lassman, H. Differentiation between Cellular Apoptosis and Necrosis by the Combined Use of *In Situ* Tailing and Nick Translation Techniques. *Laboratory Investigation*. 71(2):219, 1994.
- Gorczyca, W., Gong, J. and Darznkiewicz, Z. Detection of DNA Strand Breaks in Individual Apoptotic Cells by the *in Situ* Terminal Deoxynucleotidyl Transferase and Nick Translation Assays. *Cancer Research*. 53:1945, 1993.
- Gout, P.W., Noble, R.L. and Beer, C.T. Cultured Nb Rat Lymphoma Cells I Endocrine and Cancer Research. *Biochem. Cell Biol.* 64:659, 1986.
- Israel, A. A Role for Phosphorylation and Degredation in the Control of NFkB Activity. *T.I.G.* 11(6):203, 1995.
- Kaufmann, S.H., Quddus, F.F. and Shaper, J.H. An Alternative Approach to the Quantitation of Glucocorticoid-Receptor Complexes in the Nuclei of Lymphoid Cells. *Endocrinology*. 110(3):708.

Kerr, J.F.R. and Searle, J. A Suggested Explanation for the Paradoxically Slow Growth Rate of Basal Cell Carcinomas that Contain Numerous Mitotic Figure. *J. Pathol.* 107:41, 1972.

Kerr, J.F.R, Wyllie, A.H. and Currie, A.R. Apoptosis: A Basic Biological Phenomenon with Wide Ranging Implications in Tissue Kinetics. *Br. J. Cancer.* 26:239, 1972.

LaVoie, H.A. Investigation of Intracellular Signals Mediating the Anti-Apoptotic Action of Prolactin in Nb2 Lymphoma Cells. Ph. D. thesis. Virginia Commonwealth University, 1994.

LaVoie, H.A. and Witorsch, R.J. Investigation of Intracellular Signals Mediating the Anti-Apoptotic Action of Prolactin in Nb2 Lymphoma Cells. *P.S.E.B.M.* 209:257, 1995.

Liu, X., Robinson, G.W., Gouilleux, F., Groner, B and Hennighausen, L. Cloning and Expression of STAT5 and an Additional Homologue (STAT5b) Involved in Prolactin Signal Transduction in Mouse Mammary Tissue. *Proc. Natl. Acad. Sci. USA.* 92:8831, 1995.

McGhee, J.D. and Felsenfeld, G. Nucleosome Structure. *Ann. Rev. Biochem.* 49:1115, 1980.

Murphy, P.R., Dimattia, G.E. and Friesen, H.G. Role of Calcium in Prolactin-Stimulated c-myc Gene Expression and Mitogenesis in Nb2 Lymphoma Cells. *Endocrinology.* 122:2476, 1988.

Perry, S.W., Epstein, L.G. and Gelbard, H.A. In Situ Trypan Blue Staining of Monolayer Cell Cultures for Permanent Fixation and Mounting. *BioTechniques.* 22:1020, 1997.

Perry, S.W., Epstein, L.G. and Gelbard, H.A. Simultaneous In Situ Detection of Apoptosis and Necrosis in Monolayer Cultures by TUNEL and Trypan Blue. *BioTechniques.* 22:1102, 1997.

Picard, D. and Yamamoto, K.R. Two Signals Mediate Hormone-Dependent Localization of the Glucocorticoid Receptor. *E.M.B.O.* 6:3333, 1987.

Russel, J.H. Internal Disintegration Model of Cytotoxic Lymphocyte-Mediated Cytotoxicity. *Bio. Rev.* 56:153, 1981.

- Sadeghi, H. and Wang, S.B. Proliferation of Nb2 Lymphoma Cells in Vitro in Response to Interleukin-7. *Immunol. Lett.* 34:105, 1992.
- Scheinman, R.I., Cogswell, P.C., Lofquist, A.K. and Baldwin Jr., A.S. Role of Transcriptional Activation of I $\kappa$ B $\alpha$  in Mediation of Immunosuppression by Glucocorticoids. *Science.* 270:283, 1995.
- Schwartzman, R.A. and Cidlowski, J.A. Apoptosis: The Biochemistry and Molecular Biology of Programmed Cell Death. *Endo Reviews.* 14:133, 1993.
- Shi, Y., Sahai, B.M. and Green, D.R. Cyclosporin A Inhibits Activation-Induced Cell Death in T-Cells in Thymic Cultures. *Nature.* 339:625, 1989.
- Smith, C.A., Williams, G.T., Kingston, R., Jenkinson, E.J. and Owen, J.T. Antibodies to CD3/T-Cell Receptor Complex Induce Death by Apoptosis in Immature T Cells in Thymic Cultures. *Nature.* 337:181, 1989.
- Stocklin, E., Wissler, M., Gouilleux, F. and Groner. Functional Interactions between STAT5 and the Glucocorticoid Receptor. *Nature.* 383:726, 1996.
- Stout, L.E., Svensson, A.M. and Sorenson, R.L. Prolactin Regulation of Islet-Derived INS-1 Cells: Characteristics and Immunocytochemical Analysis of STAT5 Translocation. *Endocrinology.* 138:1592, 1997.
- Tanaka, H. and Makino, I. Ursodeoxycholic Acid-Dependent Activation of the Glucocorticoid Receptor. *Biochem. Biophys. Res. Commun.* 188(2):942, 1992.
- Tanaka, H., Makino, Y., Miura, T., Hirano, H., Okamoto, K., Komura, K., Sato, Y. and Makino, I. Ligand-Independent Activation of the Glucocorticoid Receptor by Ursodeoxycholic Acid. *J. of Immuno.* 156(4):1601, 1996.
- Tanaka, T., Shiu, R.P.C., Gout, P.W., Beer, C.T., Nobel, R.L. and Friesen, H.G. A New Sensitive and Specific Bioassay for Lactogenic Hormones; Measurement of Prolactin and Growth Hormone in Human Serum. *J. Clin. Endo. And Metab.* 51:1058, 1980.
- Telford, D.J. and Stewart, B.W. Micrococcal Nuclease: Its Specificity and Use for Chromatin Analysis. *Int. J. Biochem.* 21:127, 1989.
- Tornusciolo, D.R.Z., Schmidt, R.E. and Roth, K.A. Simultaneous Detection of TDT-Mediated dUTP-Biotin Nick End-Labeling (TUNEL)-Positive Cells and Multiple Immunohistochemical Markers in Single Tissue Sections. *BioTechniques.* 19:800, 1995.

Ucker, P.S. Death by Suicide: One Way to Go in Mammalian Cellular Development? *The New Biologist*. 3:103, 1991.

Umansky, S.R. The Genetic Program of Cell Death. Hypothesis and Some Applications: Transformation, Carcinogenesis, Ageing. *J. Theor. Biol.* 97:591, 1982.

Vedeckis, W.V. Nuclear Receptors, Transcriptional Regulation, and Oncogenesis. Society for Experimental Biology and Medicine, 1992.

Walker, N.I., Harmon, B.V., Gobe, G.C. and Kerr, J.F.R. Patterns of Cell Death. In: Kinetics and Patterns of Necrosis (Jasmin, G. ed.) S. Karger A.G., Basel, Switzerland. 18, 1988.

Wikstrom, A.N., Vakke, O., Okret, S., Bronnegard, M. and Gustafsson, J. Intracellular Localization of the Glucocorticoid Receptor: Evidence for Cytoplasmic and Nuclear Localization. *Endocrinology*. 120:1232, 1987.

Witorsch, R.J. Evidence for Human Placental Lactogen Immunoreactivity in Rat Pars Distalis. *J. of Histochemistry and Cytochemistry*. 28:1, 1980.

Witorsch, R.J., Day, B.E., La Voie, A., Hashemi, N. and Taylor, J.K. Comparison of Glucocorticoid-Induced Effects in Prolactin-Dependent and Autonomous Rat Nb2 Lymphoma Cells. *P.S.E.B.M.* 203:454, 1993.

Wyllie, A.H. Glucocorticoid-Induced Thymocyte Apoptosis is Associated with Endogenous Endonuclease Activation. *Nature*. 284:555, 1980.

Wyllie, A.H. Cell Death. *Int. Rev. Cytol.* 17(Suppl):755, 1987.

Wyllie, A.H., Kerr, J.F.R. and Currie, A.R. Cell Death: The Significance of Apoptosis. *Int. Rev. Cytol.* 68:251, 1981.

Yu-Lee, L. Molecular Actions of Prolactin in the Immune System. *P.S.E.B.M.* 215:35, 1997.

## Vita

